© 2021. Published by The Company of Biologists Ltd | Biology Open (2021) 10, bio051797. doi:10.1242/bio.051797

RESEARCH ARTICLE

Segregation of brain and organizer precursors is differentially regulated by Nodal signaling at blastula stage

Aitana M. Castro Colabianchi[1,2], María B. Tavella[3], Laura E. Boyadjián López[1,2], Marcelo Rubinstein[3,4], Lucía F. Franchini[3] and Silvia L. López[1,2,*]

ABSTRACT

The blastula Chordin- and Noggin-expressing (BCNE) center comprises animal-dorsal and marginal-dorsal cells of the amphibian blastula and contains the precursors of the brain and the gastrula organizer. Previous findings suggested that the BCNE behaves as a homogeneous cell population that only depends on nuclear β-catenin activity but does not require Nodal and later segregates into its descendants during gastrulation. In contrast to previous findings, in this work, we show that the BCNE does not behave as a homogeneous cell population in response to Nodal antagonists. In fact, we found that *chordin.1* expression in a marginal subpopulation of notochordal precursors indeed requires Nodal input. We also establish that an animal BCNE subpopulation of cells that express both, *chordin.1* and *sox2* (a marker of pluripotent neuroectodermal cells), and gives rise to most of the brain, persisted at blastula stage after blocking Nodal. Therefore, Nodal signaling is required to define a population of *chordin.1*+ cells and to restrict the recruitment of brain precursors within the BCNE as early as at blastula stage. We discuss our findings in *Xenopus* in comparison to other vertebrate models, uncovering similitudes in early brain induction and delimitation through Nodal signaling.

KEY WORDS: BCNE center, Nodal, Chordin, Gastrula organizer, Brain, Vertebrates

INTRODUCTION

When the dorsal lip of an amphibian early gastrula is grafted into the ventral side of a host, a secondary embryo develops with complete anterior-posterior and dorsal-ventral axis (Spemann and Mangold, 1924; De Robertis and Kuroda, 2004). Because of these properties, the dorsal lip region is known as the gastrula organizer (GO). The GO is preceded by an earlier dorsal signaling center, the blastula Chordin- and Noggin-expressing (BCNE) center, which expresses Chordin.1 (Chrd.1) and Noggin, two BMP antagonists proposed to initiate anterior neural induction directly in the BCNE (De Robertis and Kuroda, 2004). This center encompasses the animal/marginal dorsal cells of the blastula and gives rise to the forebrain and most of the midbrain and hindbrain, as well as to all endomesodermal tissues derived from the GO. Although *chrd.1* transcripts are distributed throughout the entire BCNE, they are restricted during gastrulation to the endomesodermal descendant of this center (GO and its derivatives) but are absent from the neuroectodermal descendant (the presumptive brain) (Kuroda et al., 2004). It was proposed that dorsal accumulation of maternal nuclear β-catenin (nβ-cat) triggers *chrd.1* expression throughout the BCNE, while Nodal signaling is only required later to maintain *chrd.1* in the GO (Wessely et al., 2001). The *siamois*-related homeobox genes (*sia*) are directly activated by the dorsal Wnt/nβ-cat cascade. They encode the first transcription factors expressed in the BCNE and activate *chrd.1* expression by directly binding to its promoter (Ishibashi et al., 2008; Reid et al., 2012). Thus, it appeared that only dorsal nβ-cat signaling initiates brain and GO development through the establishment of the BCNE, while Nodal would be required later for the maintenance of the GO and its descendants. These findings suggested that the BCNE behaves as a homogeneous cell population induced by dorsal nβ-cat and segregates later, during gastrulation, into brain and GO.

Accumulation of transcripts encoding *Xenopus* Nodal-related endomesodermal inducers (Xnrs) in the Nieuwkoop center (NC), located in the vegetal dorsal cells, requires the cooperative action of VegT and nβ-cat (Takahashi et al., 2000). Nodal activity can be experimentally blocked by the C-terminal fragment of Cerberus protein, known as Cerberus-short (Cer-S), which specifically binds to and antagonizes Xnrs (Bouwmeester et al., 1996; Piccolo et al., 1999; Takahashi et al., 2000). After blocking mesoderm induction with *cer-S* mRNA (hereafter, *cer-S*), embryos still develop head structures, including brain tissue and a cyclopic eye, express the pan-neural marker *sox2* and forebrain, midbrain, and hindbrain markers (Wessely et al., 2001). These findings indicated that anterior neural tissue can be specified in the absence of mesoderm, lending support to the idea that anterior neural specification is initiated in the BCNE due to the transient expression of neural inducers in the presumptive brain territory (De Robertis and Kuroda, 2004).

In this work, we aimed to determine if the BCNE behaves as a homogeneous or heterogeneous cell population in response to Nodal. To this end, we inhibited the Nodal pathway with *cer-S* or with a dominant-negative form of FoxH1, a transcription factor with Forkhead domain which binds Smad2 and Smad4, the transducers of Nodal signaling (Chen et al., 1997; Watanabe and Whitman, 1999; Hill, 2001). We found that the BCNE is functionally and topologically compartmentalized, as revealed by a differential

[1]Universidad de Buenos Aires. Facultad de Medicina, Departamento de Biología Celular e Histología / 1° U.A. Departamento de Histología, Embriología, Biología Celular y Genética, Laboratorio de Embriología Molecular "Prof. Dr. Andrés E. Carrasco", Buenos Aires 1121, Argentina. [2]CONICET - Universidad de Buenos Aires. Instituto de Biología Celular y Neurociencia "Prof. E. De Robertis" (IBCN), Universidad de Buenos Aires, Buenos Aires 1121, Argentina. [3]Instituto de Investigaciones en Ingeniería Genética y Biología Molecular (INGEBI) "Dr. Héctor N. Torres", Consejo Nacional de Investigaciones Científicas y Técnicas (CONICET), Buenos Aires C1428, Argentina. [4]Departamento de Fisiología, Biología Molecular y Celular, Facultad de Ciencias Exactas y Naturales, Universidad de Buenos Aires, Buenos Aires 1428, Argentina.

*Author for correspondence (slopez@fmed.uba.ar; silvialopez.emol@gmail.com)

A.M.C.C., 0000-0002-8052-8344; M.B.T., 0000-0001-5558-0717; L.E.B.L., 0000-0002-0685-8601; M.R., 0000-0002-7500-7771; L.F.F., 0000-0001-6602-2243; S.L.L., 0000-0002-3760-7549

Received 3 March 2020; Accepted 29 January 2021

Biology Open (2021) 10, bio051797. doi:10.1242/bio.051797

response of distinct cell subpopulations to the blockade of Nodal. We demonstrate that Nodal is already necessary as early as at blastula stage for restricting a subpopulation of brain precursors while favoring a subpopulation of chordal organizer precursors. We also found that during gastrulation, Nodal is required for maintaining the axial mesoderm (AM), with the chordal mesoderm (CM) being the subpopulation with highest sensitivity to Nodal depletion. Finally, we compare the requirement of Nodal signaling in the segregation of dorsal territories in *Xenopus* with those previously observed in other vertebrate models.

RESULTS

BCNE cells do not respond uniformly to Nodal blockade

We blocked Nodal by injecting *cer-S* and analyzed at s9 by *in situ* hybridization (ISH) if this could result in spatial changes of the BCNE marker *chrd.1* and its upstream regulator, the direct Wnt/nβ-cat target gene *sia1* (Ishibashi et al., 2008; Reid et al., 2012). Notably, *chrd.1* expression decreased in the marginal region of the BCNE (red asterisk, Fig. 1B) in comparison to control siblings (Fig. 1A), but persisted in the animal region (green asterisk, Fig. 1B) (Table 1). This suggests that the BCNE is composed of two *chrd.1* subdomains, regarding their response to Nodal blockade. However, the domain of the up-stream regulator *sia1* was not reduced after *cer-S* injection at any place at s9 (Fig. 1D,E, Table 1). Control experiments showed that *cer-S* significantly inhibited the expression of *mix1*, a direct target of Nodal signaling (Charney et al., 2017), both at s9 and s10 (Fig. S1A,B) and also, that of the paraxial mesoderm marker *myod1* at neurula stage (Fig. S1C,D). Our results indicate that Nodal is required for *chrd.1* expression in a subpopulation of BCNE cells, regardless of *sia1*.

Intriguingly, RT-qPCR analysis of whole embryos at s9 showed that despite that *mix1* was significantly downregulated after *cer-S* injection, as expected (Fig. S1A,B), *chrd.1* transcripts levels increased (Fig. 1C). Since this approach reflects a global measure of *chrd.1* mRNA levels and does not distinguish spatial perturbations of *chrd.1* expression within the BCNE, it is plausible that an increase in *chrd.1* transcripts levels in a subpopulation of cells masked the downregulation in another subpopulation. To corroborate if there are different *chrd.1* subdomains in the BCNE regarding Nodal regulation, we unilaterally injected *foxh1-SID* mRNA (hereafter, *foxh1-SID*), which encodes a dominant inhibitor of Smad2 activity and blocks Nodal signaling in a cell-autonomous manner (Chen et al., 1997; Müller et al., 2000). By comparing the injected- and non-injected sides at s9, we found that the animal expression of *chrd.1* persisted (green asterisk, Fig. 1F,G) but was suppressed in the marginal subdomain of the BCNE (red asterisk, Fig. 1F,G; Table 2). Control experiments showed that *foxh1-SID* suppressed the pan-mesodermal marker *tbxt* on the injected side, as expected (Fig. S1E,G).

These results confirm that the BCNE is already compartmentalized into two *chrd.1* subdomains: 1) an animal subdomain, which persists after blocking Nodal, and 2) a marginal subdomain, which depends on Nodal. This finding is in contrast to a previous proposal which stated that Nodal is not necessary for *chrd.1* expression in the BCNE and it is only required later for its maintenance in the GO (Wessely et al., 2001).

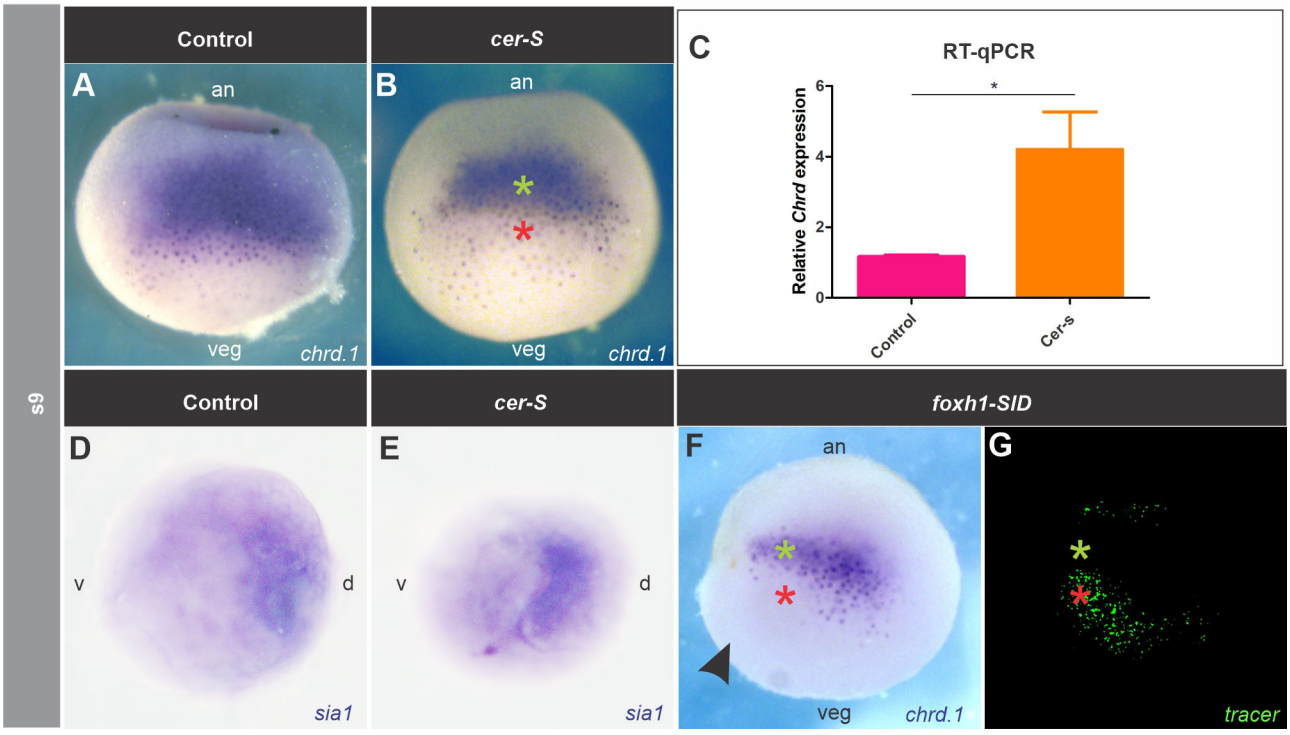

Fig. 1. Effects of blocking Nodal on *chrd.1* (A–C, F,G) and *sia1* expression (D,E) at late blastula (s9). *Chrd.1* (A) and *sia1* (D) are normally expressed in the whole BCNE center. *Cer-S* (B) and *foxh1-SID* (F,G) injections revealed a marginal BCNE subpopulation of cells that depends on Nodal to express the neural inducer *chrd.1* (red asterisk), while its upstream regulator *sia1* (E), a direct Wnt/nβ-cat target, and the animal *chrd1+* subdomain in the BCNE (B,F, green asterisk), do not depend on Nodal. The *foxh1-SID*-injected side is evidenced by the tracer's fluorescence (G) and is indicated by a black arrowhead. (C) RT-qPCR analysis showed a significant increase (P<0.05) in the levels of *chrd.1* transcripts as a result of *cer-S* injection (P=0.027, unpaired, two-tailed *t*-test) when compared with uninjected siblings. Bars represent mean+s.e.m. of six biological replicates. A,B,F,G, dorsal views; D,E, animal views; an, animal; veg, vegetal; d, dorsal; v, ventral.

Biology Open (2021) 10, bio051797. doi:10.1242/bio.051797

Table 1. Effects of *cer-S* on markers of BCNE and its derivatives (GO, DML, neural ectoderm), pan-mesoderm (*tbxt*/*bra*), and paraxial mesoderm (*myod1*)

Expression domain	Marker	Stage	Result	*n*	*N*
BCNE, animal cells	*chrd.1*	Late blastula	Persisted: 32	34	3
BCNE, marginal cells			Decreased: 32		
GO, more external cells (presumptive, pre-involuted CM)		Early gastrula	Decreased: 39	41	3
GO, deeper cells (presumptive, involuted PM)			Persisted: 39		
DML, PM		Late gastrula	Persisted: 17	18	1
DML, CM			Abolished /+cells arrested at the blastopore: 13		
BCNE, presumptive PM	*gsc*	Late blastula	Persisted: 15	15	2
GO/DML, PM		Gastrula	Decreased: 12	19	2
DML, CM	*tbxt (bra)*	Gastrula	Abolished: 68	74	4
			Decreased: 3		
GO, ring's dorsal subdomain			Abolished: 22		
			Decreased 12		
Ventrolateral mesoderm			Abolished: 8		
			Decreased: 1		
BCNE, presumptive CM	*not*	Late blastula	Decreased: 25	25	2
Lateral subdomains			Persisted: 23		
DML, CM		Gastrula	Decreased: 50	57	3
GO, ring's dorsal subdomain			Decreased: 26		
Limit of involution			Decreased: 13		
BCNE	*sia1*	Late blastula	Persisted: 32	32	3
Presumptive neural ectoderm	*sox2*	Late blastula	Persisted and increased: 52	52	2
Neural ectoderm		Gastrula	Persisted: 65	66	3
Paraxial mesoderm	*myod1*	Neurula	Abolished: 8	20	2
			Decreased: 10		

Spatial expression was analyzed by ISH. Results are expressed as the total number of embryos showing the indicated effect on each marker. DML, dorsal midline; *n*, number of injected embryos; *N*, number of independent biological replicates.

To corroborate that during s9 *chrd.1* transcripts are indeed found in the animal region fated to become neural ectoderm, we compared single ISH of *chrd.1* in whole and hemisected embryos at s9 with double ISH of *chrd.1* combined with *hes4* at s9 and s10 (Fig. 2). At these stages, the strongest expression of *hes4* is found throughout the animal hemisphere (Aguirre et al., 2013). At s9, *chrd.1* is expressed in a large dorsal domain encompassing cells in the dorsal blastocoel roof, sometimes almost reaching the animal pole, well invading the *hes4* domain, as well as in dorsal marginal zone cells (Fig. 2A–D). In contrast, at the onset of gastrulation (s10), *chrd.1* expression does not overlap the *hes4* domain in the animal hemisphere, being restricted to the dorsal marginal zone (Fig. 2D). Therefore, at s9, *chrd.1* is expressed in derivatives of both the A1 and B1 blastomeres of the 32-cell stage (Fig. 2E), which are known to contribute mainly to the neural plate and the GO, respectively (Bauer et al., 1994). This large expression of *chrd.1* at s9 encompassing both animal and marginal cells that defines a BCNE region is consistent with previous findings (De Robertis and Kuroda, 2004; Kurth et al., 2005; Harata et al., 2019).

Mesodermal derivatives of the BCNE display a differential response to Nodal blockade

We next analyzed the consequences of blocking Nodal on *chrd.1* expression during gastrulation, when it is not expressed anymore in brain precursors but persists in the GO and in its AM descendants. At early gastrula, the presumptive prechordal mesoderm (PM), which is the first to involute, occupies a relatively more internal position than the pre-involuted, presumptive CM, and both express *chrd.1* (Zorn et al., 1999; Kaneda and Motoki, 2012). At this stage, we found a less dense ISH staining for *chrd.1* in *cer-S*-injected embryos in comparison to uninjected control siblings (Fig. 3A–C). *Chrd.1* was downregulated or suppressed from more external GO cells, which correspond to pre-involuted prospective CM at the beginning of gastrulation. As these cells became more transparent due to the suppression of *chrd.1* staining, we could observe that *chrd.1* expression persisted in a cloud below them (Fig. 3B,C, Table 1). This deeper expression, more refractory to *cer-S*, corresponds to the presumptive, involuted PM at this stage. Unilateral injection of *foxh1-SID* (0.25 ng to 1 ng) allowed a better comparison of the behavior of these subpopulations between the injected and the non-injected sides. *Chrd.1* persisted (green asterisk, Fig. 3G,I) or the domain was even expanded (light blue asterisk, Fig. 2H) in the deeper, involuted cells (Table 2), while in the pre-involuted, more external cells, *chrd.1* was suppressed (red asterisk, Fig. 3G–I, Table 2). To corroborate the contribution of *chrd*+ cells to PM and CM, we analyzed the expression of this marker at s13. Normally, at this stage, all *chrd*+ cells have been internalized, and PM and CM have

Table 2. Effects of *foxh1-SID* on the spatial expression of *chrd.1* in the BCNE and the GO

Expression domain	Marker	Stage	Results	*n*	*N*
BCNE, animal cells	*chrd.1*	Late blastula	Persisted: 32	36	2
BCNE, marginal cells			Decreased: 32		
GO, more external cells (presumptive, pre-involuted CM)		Early gastrula	Decreased: 52	54	4
GO, deeper cells (presumptive, involuted PM)			Persisted: 52		

Expression was analyzed by ISH. Results are expressed as the total number of embryos showing the indicated effect on chrd.1. *n*, number of injected embryos; *N*, number of independent biological replicates.

Biology Open (2021) 10, bio051797. doi:10.1242/bio.051797

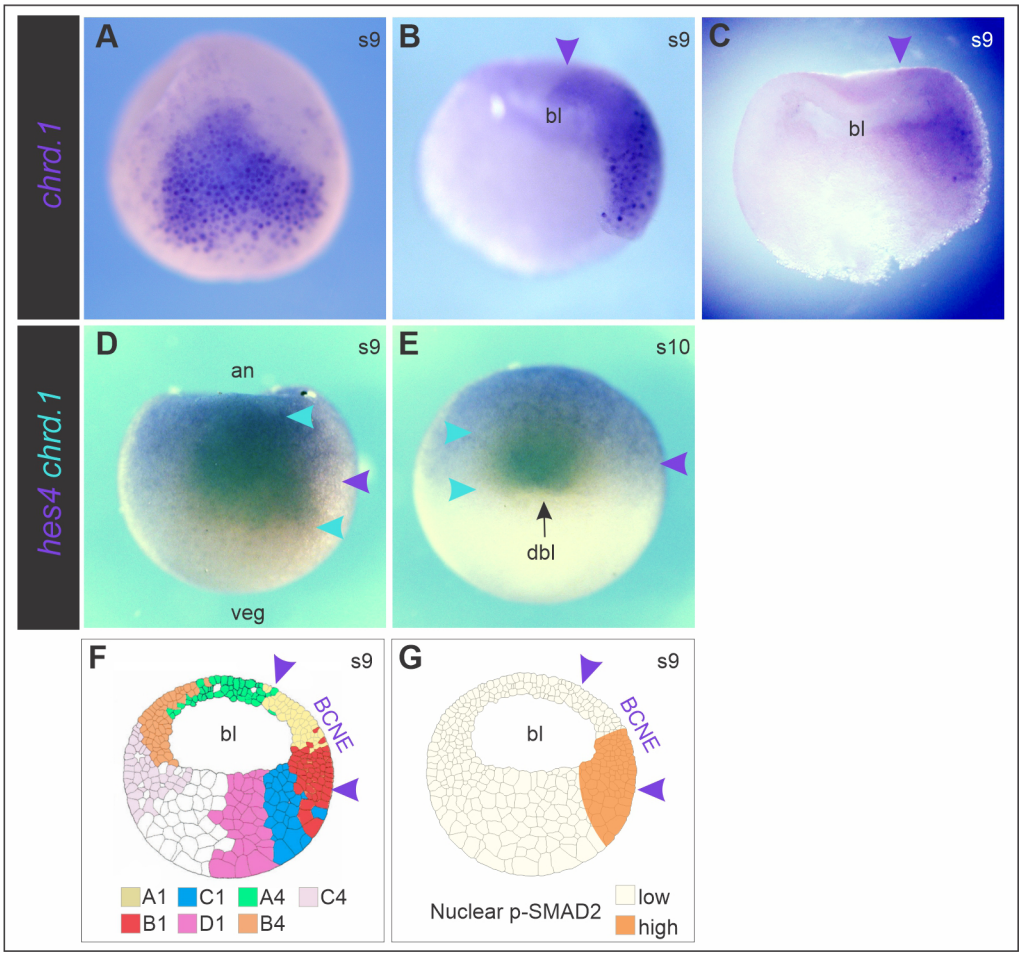

Fig. 2. *chrd.1* expression invades the animal hemisphere during s9 and is later restricted to the gastrula organizer. (A–C) ISH of *chrd.1* at s9 in a whole embryo (A) and in two different hemisected embryos obtained from an independent female (B,C). Notice the large domain of *chrd.1* encompassing both animal and marginal dorsal cells. Arrowheads in B,C point to the animal limit of *chrd.1* expression, near the animal pole. (D,E) Double ISH for *chrd.1* (revealed with BCIP, cyan) and *hes4* (revealed with NBT+BCIP, purplish) at s9 (D) and s10 (E). At these stages, the strongest *hes4* expression is found throughout the animal hemisphere, as previously shown (Aguirre et al., 2013). Purple arrowheads in D,E point to the approximate limit of this strong animal *hes4* domain. A large *chrd.1* domain readily invades the animal hemisphere at s9 (cyan arrowheads), overlapping *hes4* in the animal region, almost reaching the animal pole. At the onset of gastrulation (s10), *chrd.1* does not overlap *hes4* expression in the animal hemisphere, being restricted to the dorsal marginal zone (cyan arrowheads) (E). (F) Color-coded diagram illustrating the contribution of A1 to C4 blastomeres from the 32-cell stage embryo to the s9 stage embryo (modified from Bauer et al., 1994). *chrd.1* expression in the BCNE region (between purple arrowheads) comprises both A1 and B1 derivatives. The GO mostly derives from B1 whereas A1 mainly contributes to the neural plate (Bauer et al., 1994). (G) Distribution of nuclear phosphorylated-SMAD2 (p-SMAD2) at s9, showing that Nodal signaling is highly transduced in the dorsal-marginal and dorsal vegetal region at late blastula but not in the animal part of the BCNE area modified from Schohl and Fagotto (2002). Illustrations of midsagittal sections of s9 embryos in F,G based on Hausen and Riebesell (1991). an, animal; veg, vegetal; bl, blastocoel cavity; dbl, dorsal blastopore lip.

completely segregated. This allows the distinction of two *chrd*+ subdomains in the AM, with clear distinct shapes: a) an anterior fan-like subdomain, characterized by an active migration behavior, corresponding to the PM (green arrow, Fig. 3D); b) a posterior subdomain, corresponding to the notochordal cells (red arrow, Fig. 3D), which ultimately form a rod by convergent-extension movements (Murgan et al., 2014; Kwan and Kirschner, 2003). *Cer-S*-injected embryos showed that most *chrd.1* expression consisted of the fan-shaped subdomain (green arrow, Fig. 3E,F). In contrast, the posterior subdomain was lost or reduced (red arrows, Fig. 3E,F), sometimes with *chrd.1*+ cells arrested on the blastopore, unable to involute (yellow asterisk, Fig. 3E) (Table 1).

It was previously shown that not all the PM express *chrd.1* in *Xenopus* (Yamaguti et al., 2005). These authors showed that the PM consists of two cell populations, a more anterior one (APM) expressing the homeodomain transcription factor Goosecoid (Gsc), and a more posterior one (PPM) expressing *chrd.1* (Yamaguti et al., 2005). The same occurs in the mouse (Anderson et al., 2002). Therefore, we analyzed the consequences of *cer-S* injection on the spatial expression of *gsc* and of the CM-specific transcription factor Tbxt/Brachyury, which control the characteristic movements of PM and CM cells, respectively, in an antagonistic way (Artinger et al., 1997; Latinkić and Smith, 1999; Kwan and Kirschner, 2003; Luu et al., 2008). Our ISH results show that, at gastrula stages, *gsc* expression decreased in most *cer-S*-injected embryos (Fig. 4D,E) (Table 1). We also found through RT-qPCR analysis that *gsc* was downregulated at the onset of gastrulation after overexpression of *cer-S* (Fig. 4F). ISH analysis showed that *tbxt* was affected at different degrees. The expression normally found in the extending notochord (red arrows, Fig. 5A,C,E) was suppressed in almost all injected embryos (Fig. 5B,D,F,G, Table 1). The expression in the

Biology Open (2021) 10, bio051797. doi:10.1242/bio.051797

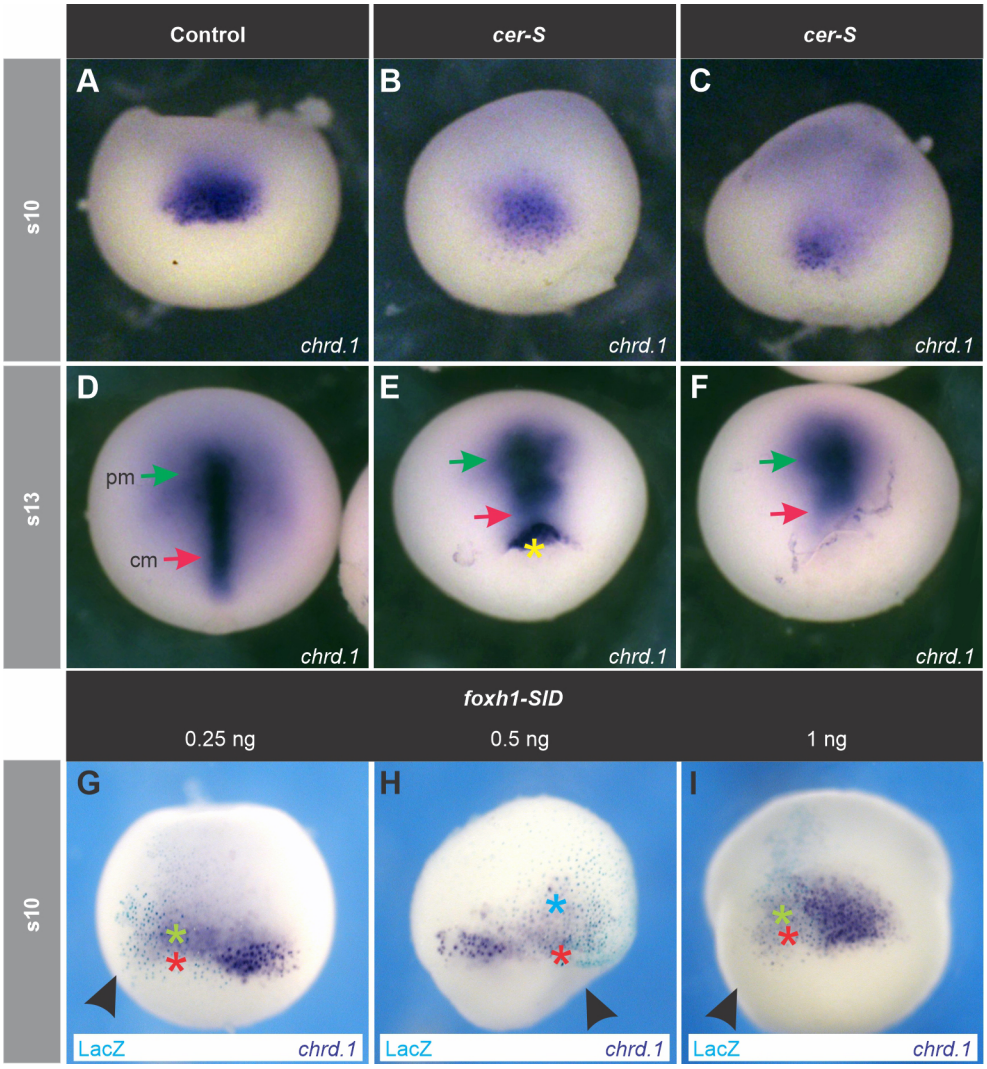

Fig. 3. Effects of blocking Nodal on *chrd.1* expression during gastrulation. (B,C,E,F) Injection of *cer-S*. (G–I) Unilateral injection of *foxh1-SID*. (A,D) Uninjected control siblings of embryos shown in B,C and E,F, respectively. At early gastrula (s10), *chrd.1* is expressed in the more external, pre-involuted presumptive CM cells and in the deeper, involuted presumptive PM, which are seen together as a compact domain (A, and non-injected side in G–I), but ceases expression in brain precursors (Kuroda et al., 2004). *cer-S* (B,C) and *foxh1-SID* (G-I) suppressed *chrd.1* expression in the pre-involuted population (red asterisks, G–I), but did not affect (green asterisks, G–I) or even expanded (light blue asterisk, H) *chrd.1*+ cells in the involuted population. The *foxh1-SID*-injected side is evidenced by X-gal turquoise staining (G–I) and is indicated by black arrowheads. At late gastrula (s13), *chrd.1* is expressed in the PM (green arrow, D) and the CM (red arrow, D). In *cer-S*-injected embryos, PM *chrd.1* expression persisted (E,F, green arrows) but CM expression decreased (E,F, red arrows) or was arrested at the blastopore (E, yellow asterisk). All embryos are shown in dorsal views, anterior side upwards.

GO presumptive mesoderm (dorsal part of the *tbxt* ring, yellow asterisk, Fig. 5A,C,E) often disappeared or was downregulated (Fig. 5B,D,F, Table 1) and that of the non-GO presumptive mesoderm (white arrows, Fig. 5A,C,E) was sometimes suppressed (Fig. 5B,G, Table 1). As an independent notochordal marker, we also analyzed the spatial expression of *not*, which encodes a homeodomain transcription factor normally expressed during gastrulation in the extending CM, GO, and in the limit of involution (von Dassow et al., 1993). *cer-S* injections affected the *not* pattern in a similar way to *tbxt* (Fig. 5H–M, Table 1). These observations indicate that, during gastrulation, among the mesodermal descendants, CM cells are the most sensitive to Nodal blockade, which disrupted notochord development almost completely. Although cells with PM characteristics persisted, as shown by ISH of *chrd.1*, a lower *gsc* expression was detected at gastrula stages, both by ISH and by RT-qPCR. This might be due to a differential sensitivity among APM and PPM subpopulations to Nodal blockade. In addition, the ventrolateral mesoderm was less sensitive to *cer-S* than the CM, as shown by a lower penetrance of the downregulation of *tbxt* in the circumblastoporal ring.

In conclusion, Nodal is required for the onset of *chrd.1* expression in the marginal subdomain of the BCNE at the blastula stage. Later, the mesodermal descendants of the BCNE require Nodal for their maintenance during gastrulation, with the CM having the highest requirement.

Nodal restricts neural specification and is required for the expression of CM but not of PM markers at the BCNE stage

We have observed that blocking Nodal distinguishes two *chrd.1*+ subpopulations in the BCNE. Since this center is composed of the brain and GO precursors, and the GO, in turn, segregates into PM and CM, we wondered if blocking Nodal could already discriminate between PM and CM precursors and the neural ectoderm at s9. For this purpose, we compared the expression of the pan-neural marker *sox2* and the specific PM (*gsc*) and CM (*not*) markers in the BCNE between *cer-S*-injected embryos and uninjected control siblings at s9. Although it is known that *gsc* and *tbxt* are involved in an antagonistic relationship that controls PM and CM segregation during gastrulation (Artinger et al., 1997; Latinkić and Smith, 1999; Kwan and Kirschner, 2003; Luu et al., 2008), *tbxt* is weakly expressed in the presumptive CM at late blastula. Therefore, we chose *not* as an alternative spatial marker of CM precursors. While *gsc* and *sox2* expression persisted and even increased in the case of the latter (Fig. 4A–C,G–I, Table 1), *not* expression in the BCNE subdomain corresponding to the presumptive CM territory decreased in *cer-S*-injected embryos (Fig. 4H,I, Table 1). Interestingly, RT-qPCR analysis showed that

Biology Open (2021) 10, bio051797. doi:10.1242/bio.051797

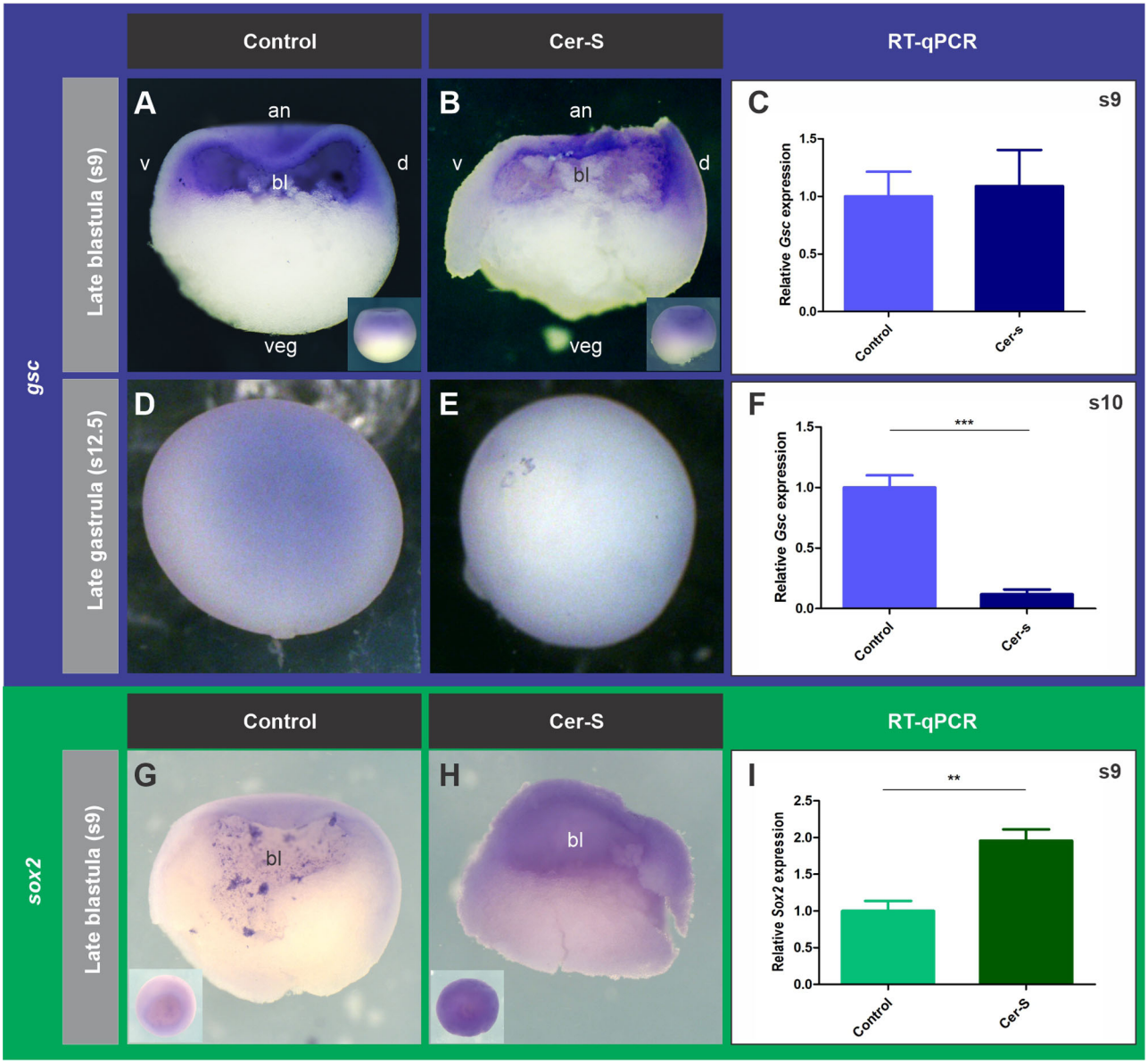

Fig. 4. Effects of *cer-S* on the PM marker *gsc* (A–F) and the neural marker *sox2* (G–I) at the stages indicated. (A–C) After *cer-S* injection, *gsc* expression was not significantly affected at s9, as revealed by ISH (A,B) and RT-qPCR (C) (P=0.8184; unpaired, two-tailed *t*-test) when compared with uninjected siblings. Bars represent mean+s.e.m. of six biological replicates. (D–F) At the end of gastrulation, *gsc* expression decreased in the PM of most *cer-S*-embryos injected, as revealed by ISH (D,E). *Gsc* transcripts levels were also significantly reduced at s10 (P<0.05), as revealed by RT-qPCR (F) (P=0.0002; unpaired, two-tailed *t*-test) when compared with uninjected siblings. Bars represent mean+s.e.m. of four biological replicates. (G) Control blastula showing expression of the neural marker *sox2*, which was consistently increased in *cer-S*-injected siblings, as revealed by ISH (H). A significant increase (P<0.05) in *sox2* transcripts levels was detected by RT-qPCR at s9 in *cer-S*-injected embryos (P=0.0016; unpaired, two-tailed *t*-test) when compared with uninjected siblings (I). Bars represent mean+s.e.m. of five biological replicates. (A,B,G,H) Sagittal hemisections of s9 embryos; insets in A,B show dorsal views of whole embryos; insets in G,H show animal views of whole embryos; (D,E) dorsal views. an, animal; veg; vegetal; d, dorsal; v, ventral; bl, blastocoel cavity.

both, *chrd.1* and *sox2* expression at s9 increased after blocking Nodal (Figs 1C and 4I). These results indicate that the population of brain precursors expressing both, the neural inducer and the neural specification marker in the BCNE was expanded after blocking Nodal. Also, because the animal *chrd.1* subdomain was essentially refractory to the blockade of Nodal signaling, while the marginal subdomain was suppressed, as shown by ISH (Fig. 1A,B, F,G), an increase in the level of *chrd.1* transcripts in neural precursors might account for the global increase measured by RT-qPCR at s9 (Fig. 1C).

Thus, we propose that BCNE cells are functionally compartmentalized, with presumptive CM cells requiring Nodal for their specification, while neural specification is restricted by Nodal.

A revised model for the requirement of Nodal signaling at blastula and gastrula stages and the delimitation of brain precursors and GO-derived populations

The results presented here indicate that Nodal is indeed required to trigger the full expression of the neural inducer *chrd.1* in the BCNE

Biology Open (2021) 10, bio051797. doi:10.1242/bio.051797

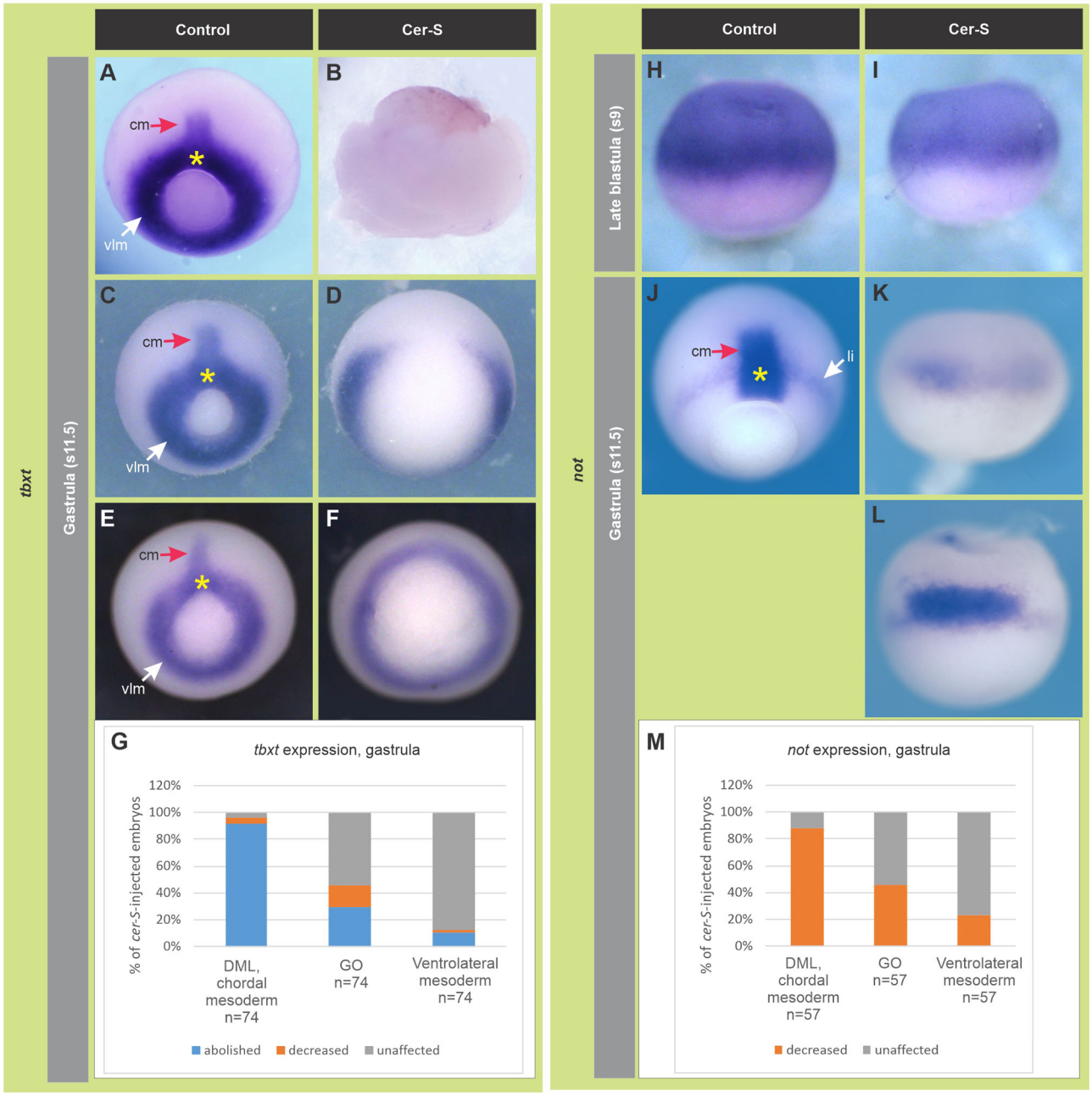

Fig. 5. Effects of *cer-S* on the spatial expression of the pan-mesoderm/CM marker *tbxt* (A–G) and the CM marker *not* (H–M) at the stages indicated in grey boxes. (A,C,E) Control gastrulae showing *tbxt* expression in the CM (red arrow), GO (yellow arrow) and presumptive ventrolateral mesoderm in the blastopore (vlm, white arrow). (B,D,F) *cer-S*-injected embryos which are siblings of those shown in A,C,E, respectively. (G) Summary of the effects of *cer-S* on *tbxt* expression at gastrula stage. Results are expressed as the percentage of embryos showing the indicated phenotypes for each *tbxt* subdomain. (H) Dorsal view of a control late blastula, showing strong *not* expression in the BCNE region, which decreased in *cer-S*-injected siblings (I). (J) Control gastrula showing *not* expression in the extending CM (red arrow), GO (yellow asterisk) and limit of involution (li, white arrow). *Cer-S* abolished *not* expression in the extending notochord (K,L,M) and often decreased it in the GO (K,M); when *not* expression was not decreased in the GO (L), *not+* cells were arrested at the blastopore, unable to involute. (M) Summary of the effects of *cer-S* on *not* expression at gastrula stage. Results are expressed as the percentage of embryos showing the indicated phenotypes for each *not* subdomain. See main text for details. (A–F,J) Posterior/dorsal views. (H,I,K,L) Dorsal views.

(Fig. 6C), in contrast to a previous proposal (Wessely et al., 2001) (Fig. 6A,B). In fact, we found that *chrd.1* was abolished by either *cer-S* or *foxh1-SID* in the marginal region of this center, whereas *sox2* expression increased at s9 in *cer-S*-injected embryos. These results indicate that the population of brain precursors in the BCNE was expanded after blocking Nodal. Indeed, we notice that the *chrd.1* domain in *cer-S*-injected embryos at s9 (shown in Fig. 3D,E in Wessely et al., 2001) is less extended in the animal-vegetal axis in comparison to control siblings, resembling the results shown in the present work, but the authors interpreted that *chrd.1* expression was refractory to the blockade of Nodal. Besides, we found that the PM marker *gsc* persisted whereas the notochordal marker *not* was reduced in the BCNE after blocking Nodal. Therefore, mesodermal precursors in the BCNE are differentially regulated by Nodal.

Altogether, these results indicate that the BCNE does not behave as a homogeneous cell population. In fact, our data show that the

Biology Open (2021) 10, bio051797. doi:10.1242/bio.051797

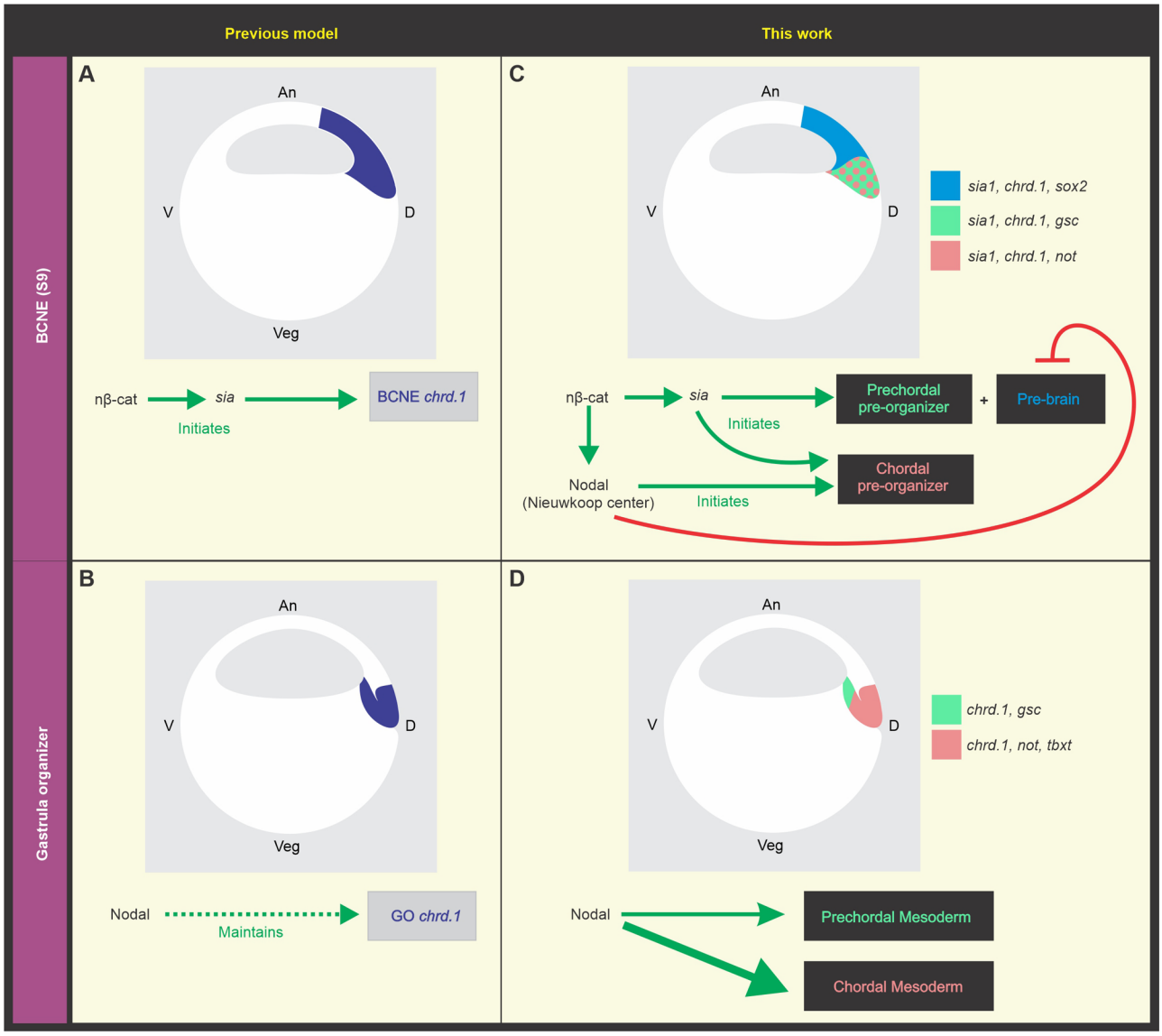

Fig. 6. (A,B) Previous model of Wnt/nβ-cat and Nodal requirements for *chrd.1* expression in the blastula and gastrula dorsal signaling centers (Wessely et al., 2001). Dorsal nβ-cat initiates *chrd.1* expression in the BCNE through direct activation of the gene encoding the transcription factor Sia (Ishibashi et al., 2008). According to this model, Nodal signaling is not required to initiate *chrd*.1 expression in the BCNE (A), but it is later required for the maintenance of *chrd*.1 expression in the GO (B). (C,D) Role of Nodal and Wnt/nβ-cat in BCNE compartmentalization and the development of its derivatives updated in the present work. The expression domains of the markers analyzed in this study are color-coded. (C) Dorsal nβ-cat initiates pre-brain and prechordal pre-organizer induction through the activation of *sia* in the BCNE. Accumulation of *nodal* transcripts in the NC requires the cooperative action of VegT and dorsal nβ-cat (Takahashi et al., 2000). Dorsal nβ-cat initiates chordal pre-organizer induction through the activation of *sia* in the BCNE and *nodal*-related genes in the NC. (D) During gastrulation, high Nodal signaling maintains CM development, whereas low Nodal signaling maintains PM development.

BCNE is compartmentalized into the precursors of the prospective brain (pre-brain), the PM precursors, and the CM precursors, which can be distinguished earlier than previously thought since they are being differentially regulated by Nodal (Fig. 6C). Therefore, here we present a modified model of the originally proposed by Wessely et al. (2001), concluding that *chrd.1* expression is triggered in the whole BCNE by Wnt/nβ-cat through *sia* (Ishibashi et al., 2008) and has different requirements for Nodal, depending on the BCNE subpopulation. Nodal is necessary to trigger *chrd.1* expression in the chordal pre-organizer, whereas it is not required at the prechordal pre-organizer. At the pre-brain subpopulation, *chrd.1* is restricted by Nodal (Fig. 6C). Since *sia1* expression persisted in the BCNE after *cer-S* injection and *sox2* expression increased, we suggest that Nodal restricts the pre-brain territory downstream of *sia* (Fig. 6C). Besides, within the presumptive mesodermal subdomain in the BCNE (pre-organizer), Nodal promotes the development of posterior AM derivatives but does not affect the presumptive prechordal subpopulation at this stage (Fig. 6C). Later, Nodal is necessary to maintain both the CM and the PM during gastrulation. The *chrd.1*, *tbxt*, and *gsc* patterns at gastrula stages suggest that, among all mesodermal derivatives, the CM is the most sensitive to the blockade of Nodal in *Xenopus*. Thus, it appears that CM maintenance during gastrulation requires more input from Nodal than other mesodermal cell types, like the PM.

The subdivision of the BCNE into two *chrd.1* subdomains according to Nodal responsiveness shown here is consistent with the observation that, at stage 9, nuclear phosphorylated-SMAD2 (p-SMAD2), a *bonafide* indicator of active transduction of Nodal

Biology Open (2021) 10, bio051797. doi:10.1242/bio.051797

signaling, is highly accumulated in the dorsal-marginal and dorsal-vegetal region but not in the animal part of the BCNE area (Schohl and Fagotto, 2002) (Fig. 2G). Moreover, cycloheximide treatment prevented the reduction of the *chrd1* domain in early gastrulae, which showed a larger *chrd.1* domain very similar to the BCNE domain at stage 9 (Kurth et al., 2005). This indicates that during the blastula-to-gastrula transition, a mechanism dependent on protein synthesis normally represses the animal subdomain of *chrd1* expression present in the BCNE, without affecting *chrd.1* expression in the GO. This mechanism probably underlies the downregulation of *chrd.1* in the neural descendants of the BCNE during gastrulation described by Kuroda et al. (2004). Interestingly, *sia1* expression shows a dynamic patterning, first appearing in the animal and marginal region at s8/8.5, then adding a vegetal domain at early s9. By mid-stage 9, expression of *sia1* has disappeared from the animal region but persists in the marginal and vegetal regions (Sudou et al., 2012). The combined knockdown of *sia1*+*sia2* completely abolishes *chrd.1* expression in the BCNE. Therefore, the downregulation of *sia1* that normally takes place in the animal domain might underlie the disappearance of *chrd.1* expression from the neural derivatives of the BCNE at the onset of gastrulation. While Nodal and *sia* converge in the positive regulation of *chrd.1* in the marginal subdomain of the BCNE, it is not known if additional pathways, apart from the Wnt/nβ-cat/*sia* cascade, are necessary for triggering *chrd.1* expression in the animal subdomain of the BCNE.

DISCUSSION

The default-state model of neural specification adopted for *Xenopus* and mouse embryos poses that the default fate of ectoderm (epiblast) is neural, but it is actively repressed by BMP signaling. This default-state is revealed during neural induction, when the ectoderm is exposed to BMP antagonists, like Chordin and Noggin (Levine and Brivanlou, 2007). In *Xenopus*, this initial step of neural induction occurs before gastrulation in the BCNE, as the BMP antagonists are directly expressed by neuroectodermal precursors fated to give rise to the forebrain (Kuroda et al., 2004). Like in *Xenopus* at the blastula stage (this work, Fig. 7A), the first neural tissue induced in mouse expresses the pan-neural marker Sox2 (Levine and Brivanlou, 2007). Moreover, this neural tissue initially has a forebrain character, but it is subsequently posteriorized during gastrulation to form the rest of the central nervous system (CNS) (Levine and Brivanlou, 2007) (Fig. 7I,J). However, unlike *Xenopus*, Chrd and Noggin are not expressed before gastrulation in the mouse. Chrd transcripts first appear in the GO at the mid-streak stage (Anderson et al., 2002; Kinder et al., 2001) (Fig. 7K). Noggin appears later in the GO, and both genes are expressed in the GO-derived AM (Fig. 7L) (McMahon et al., 1998; Bachiller et al., 2000), but they were not detected in the prospective forebrain, unlike in the *Xenopus* BCNE (Fig. 7A–C) (Kuroda et al., 2004). Therefore, the default model for anterior neural induction in mice implied that the source of BMP antagonists lies in the GO and its derived tissues (Levine and Brivanlou, 2007), i.e. outside the presumptive forebrain. However, we note that transcripts from a Chordin-like1 gene (Chrdl1) are first detected in the future neural plate at E7.0 in mice (Fig. 7K) and persist there during gastrulation (Fig. 7L) (Coffinier et al., 2001). Notably, Chrdl1 never appears in the node or the primitive streak (PS), thus establishing a complementary pattern in relation to Chrd1 (Fig. 7K,L) (Coffinier et al., 2001). Chrdl1 behaves as a BMP antagonist (Sakuta et al., 2001; Chandra et al., 2006) and mouse Chrdl1 was more potent than *Xenopus chrd.1* in the induction of complete secondary axes in frogs (Coffinier et al., 2001). Thus, as early as at E7.0 [when a range of pre-streak to mid-streak embryos can be obtained, according to EMAP eMouse Atlas Project (http://www.emouseatlas.org)] the mouse future neural plate indeed expresses a BMP antagonist of the Chordin family. An ortholog *chrdl1* gene was identified in *Xenopus*, but transcripts were not detected before tailbud stages (Pfirrmann et al., 2014). Therefore, it seems that cells in the presumptive brain territory already express BMP antagonists as early as at late blastula in *Xenopus* (*chrd.1*) or around the onset of gastrulation in mouse (Chrdl1), when the anterior AM just begins migrating from the early GO to completely underlie the future forebrain later in gastrulation.

Single knockout mice for Chrd or Noggin undergo normal neural induction and anterior CNS patterning (Bachiller et al., 2000; McMahon et al., 1998). Although double knockouts demonstrated that both are necessary for forebrain maintenance (Bachiller et al., 2000), it was not studied if forebrain specification, which normally takes place around the mid-streak stage (Levine and Brivanlou, 2007), effectively occurred. On the other hand, Chrdl1$^{-/-}$ mice developed a CNS and survived to adulthood (Blanco-Suarez et al., 2018). Double knockouts of Chrd and Chrdl1 should be obtained to study if both genes are necessary for neural specification.

In *Xenopus*, *chrd.1* expression in the chordal pre-organizer population requires induction by Nodal (this work, Fig. 7A). We notice that in the mid-streak stage mouse, while Nodal is strongly expressed in the posterior-proximal quadrant of the epiblast, where the PS forms and endomesoderm ingression takes place (Varlet et al., 1997) (Fig. 7K), Chrdl1 is oppositely expressed with the highest levels in the anterior quadrant (Coffinier et al., 2001) (Fig. 7K), where anterior neural specification is taking place (Fig. 7I). This pattern resembles the complementary expression of *Xenopus chrd.1* and *nodal* genes in the BCNE/prospective brain and the NC (dorsal endoderm), respectively (Fig. 7A). However, it was not studied if Nodal normally controls mouse Chrdl1.

Remarkably, Nodal$^{-/-}$ embryos showed an expanded and premature specification of neural ectoderm expressing forebrain markers in the epiblast (including the rostral forebrain regulator Hesx1), and Gsc expression persisted in the future GO region at pre-streak stages (Camus et al., 2006). When examined at streak-stages, Nodal$^{-/-}$ embryos did not develop a morphologically distinguishable PS, and Gsc expression was always absent. Interestingly, Tbxt expression was also absent, except for some caudal cells in around 10% of mutant embryos. Moreover, some patches of other caudal mesoderm markers were present in 25% of mutant embryos (Conlon et al., 1994). FoxH1$^{-/-}$ embryos neither expressed Gsc nor Foxa2 at the anterior tip of the PS during gastrulation and failed to form a definitive node and notochord (Yamamoto et al., 2001; Hoodless et al., 2001). Surprisingly, neither Chordin nor Noggin expression was analyzed in Nodal knockouts. However, conditional removal of Smad2 activity from the epiblast or deletion of the proximal epiblast enhancer (PEE) of the Nodal gene (which renders attenuated expression of Nodal in the PS) neither suppressed node formation nor anterior neural specification. However, Gsc expression corresponding to the prechordal plate was lost at the late-streak stage in both mutants, while Chordin and Noggin expression was aberrant and decreased along the axial midline in Smad2 mutants (it was not analyzed in Nodal-PEE mutants) (Vincent et al., 2003). Therefore, Gsc expression in the mouse AM region also appears to display two phases concerning Nodal responsiveness, like those we show here for *Xenopus*: an earlier one (before PS formation) in the future GO region, which does not depend on Nodal (Camus et al., 2006), and a later one, in the node/prechordal plate, which requires Nodal (Conlon et al., 1994; Yamamoto et al., 2001; Hoodless et al., 2001; Vincent et al., 2003). Overall, these results in mouse resemble

Biology Open (2021) 10, bio051797. doi:10.1242/bio.051797

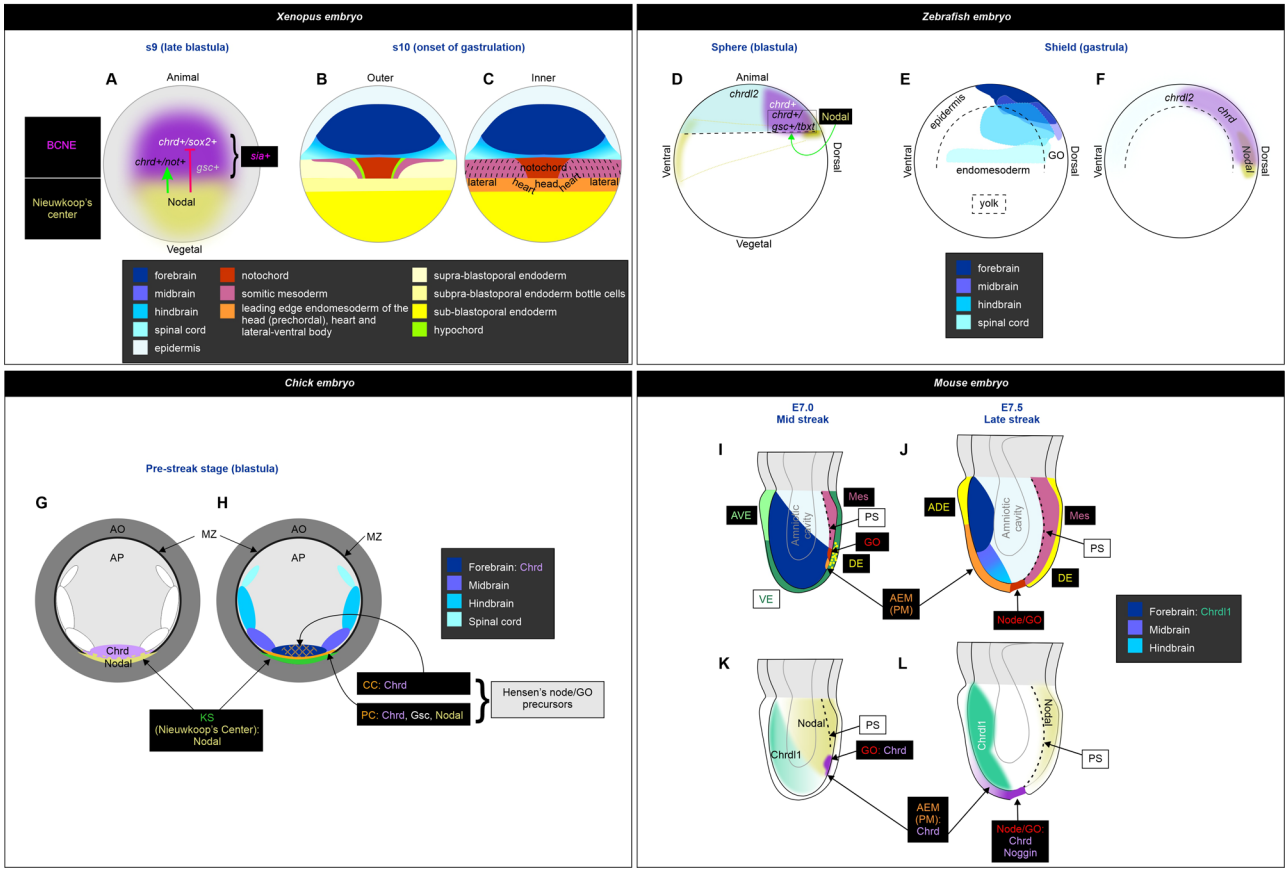

Fig. 7. Comparison between vertebrate models. (A) Position of the dorsal signaling centers at the blastula stage in *Xenopus* (dorsal view). Expression patterns were obtained from the following sources: *chrd.1* (Kuroda et al., 2004); *gsc* (Sudou et al., 2012); *nodal* (Agius et al., 2000; Takahashi et al., 2000; Kuroda et al., 2004; Reid et al., 2016); *sia* (Sudou et al., 2012); *sox2* (this work). While *sia* is expressed in the whole BCNE, *gsc* transcripts are present in a subset of BCNE cells (Sudou et al., 2012), and its expression is not perturbed by blocking Nodal (this work). The presence of different cell subpopulations in the BCNE is shown according to the response of the indicated markers to Nodal. The green arrow denotes that Nodal favors the specification of subpopulations expressing *chrd.1* and *not* (black letters) and does not necessarily imply direct regulation of these genes. The red broken line denotes that Nodal restricts the specification of the subpopulations expressing *chrd* and *sox2* (white letters) and does not necessarily imply direct regulation of these genes. (B,C) Fate map of the outer (A) and inner (B) cell layers of *Xenopus* at the onset of gastrulation (dorsal view), just before the beginning of endomesoderm internalization (adapted from Keller, 1975; Keller, 1976; Shook and Keller, 2004; Shook et al., 2004). A high-resolution fate map of s9 *Xenopus* embryos is not available, but lineage tracing experiments demonstrated that the BCNE gives rise to the forebrain and part of the midbrain and hindbrain (neurectoderm derivatives) and to the AM and floor plate (GO derivatives) (Kuroda et al., 2004). Therefore, a rough correlation of the predicted territories can be projected from the s10 map to the s9 embryo. (D) Diagram of a sphere stage zebrafish embryo, showing the expression patterns of the following markers: *chrd* (Sidi et al., 2003; Branam et al., 2010); *chrdl2* (Branam et al., 2010); *nodal1 (squint)+nodal2 (cyclops)* (Feldman et al., 1998; Rebagliati et al., 1998). The presence of different cell subpopulations in the blastula dorsal signaling center are shown according to the response of the indicated markers to Nodal. The green arrow denotes that Nodal favors the specification of subpopulations expressing *chrd* and *gsc* (black letters) and does not necessarily imply direct regulation of these genes. Another subpopulation of *chrd*+ cells (white letters) does not require Nodal at blastula stage. (E) Fate map for the zebrafish CNS at the shield stage. (F) *Chrd*, *chrdl2* and *Nodal* expression in zebrafish at shield stage (bibliographic references as in D). The broken line depicts the limit of the yolk cell. (G,H) Diagram illustrating a pre-streak stage chick embryo, showing Chrd and Nodal expression (G) and a rough fate map for the precursors of the CNS and GO (H). Predictions of the locations of the centers of the prospective territories of the CNS are shown in a gradient of blue colors, as there is a great overlap of cell fates at this stage (modified from Stern et al., 2006; Foley et al., 2000). The PC and CC contributing to Hensen's node are also shown (modified from Streit et al., 2000). Expression patterns were obtained from the following sources: Chrd (Streit et al., 1998; Matsui et al., 2008); Nodal (Matsui et al., 2008); Gsc (Izpisúa-Belmonte et al., 1993). Notice the proposed overlap in the territories of the prospective forebrain (dark blue) and a subset of the GO precursors (stippled orange), both expressing Chrd, which is also expressed by another population of GO precursors (PC) that also expresses Gsc. AO, area opaca; AP, area pellucida; KS, Köller's sickle (located in the superficial part of the posterior marginal zone); GO, Hensen's node; MZ, marginal zone. (I,J) Gastrulating mouse embryos at mid- (I) and late-streak (J) stages, respectively, indicating signaling centers and embryological regions. Illustrations were based on the following sources: (Tam and Behringer, 1997; Tam et al., 1997; Beddington and Robertson, 1999; Kinder et al., 2001; Yamaguchi, 2001; Tam and Rossant, 2003; Levine and Brivanlou, 2007; Shen, 2007). ADE, anterior definitive endoderm; AEM, anterior endomesoderm; AVE, anterior visceral endoderm; GO, gastrula organizer; Mes, mesoderm; PM, prechordal mesoderm; PS, primitive streak (broken line); VE, visceral endoderm. Blue colors represent the progressive anterior-posterior regionalization of the neural ectoderm in the model for anterior neural induction/posteriorization proposed by Levine and Brivanlou (2007). (K,L) Expression patterns at mid (K) and late (L) streak stages were obtained from the following sources: Chrd, (Bachiller et al., 2000); Chrdl1, (Coffinier et al., 2001); Nodal, (Varlet et al., 1997; Shen, 2007).

our findings after blocking Nodal in *Xenopus*, indicating that this pathway is required for restricting forebrain induction before gastrulation (Camus et al., 2006), for the maintenance of PM cells during gastrulation, and for the development of notochordal cells (Conlon et al., 1994; Yamamoto et al., 2001; Hoodless et al., 2001; Vincent et al., 2003). However, the development of a subset of

Biology Open (2021) 10, bio051797. doi:10.1242/bio.051797

posterior mesodermal cells does not show a high dependency on Nodal in both, mouse (Conlon et al., 1994) and *Xenopus* (this work). These observations suggest that in amphibians and mammals, before overt signs of gastrulation, Nodal is not necessary for the initial specification of the prechordal pre-organizer, but as gastrulation progresses, Nodal is required for the maintenance of the GO, the PM, and the notochord.

In conclusion, while in *Xenopus*, the same gene (*chrd.1*) is expressed in both pre-brain and pre-organizer territories in the BCNE (Fig. 7A), separate mouse genes encoding BMP antagonists belonging to the Chordin family are expressed in the presumptive neural plate (Chrdl1) and the GO (Chrd1) (Fig. 7K,L). In *Xenopus*, Nodal differentially regulates *chrd.1* among the BCNE cells, being necessary for the initiation of *chrd.1* expression in the presumptive CM subpopulation and to restrict that of the pre-brain subpopulation. In mice, it is not known if Nodal analogously restricts Chrdl1 expression in the presumptive brain territory, although their complementary expression patterns suggest so. The SMAD2 conditional knockout indicates that Nodal is also necessary for Chrd1 expression during gastrulation in mice, although it is not known if it is required for its initial expression in the GO or its maintenance since the analysis was performed at headfold stage (Vincent et al., 2003).

In chick embryos, the posterior marginal zone (PMZ) was proposed as the NC equivalent (Joubin and Stern, 2001) (Fig. 7G, H). The Köller's sickle (KS) is a crescent-shaped region of the superficial portion of the PMZ (Stern, 1990) (Fig. 7H). Two cell populations that contribute to the chick GO (Hensen's node) were identified before the onset of gastrulation. One is initially located in the epiblast, just above the anterior face of KS at stage X, and moves anteriorly between stages XI and XIII to the center of the blastoderm. These are known as central cells (CC) (Fig. 7H). The second group, known as posterior cells (PC), is located within the middle layer and is initially associated with the inner face of KS (Fig. 7H). These PC start expressing Gsc before gastrulation and migrate later than the CC, within the middle layer, together with the tip of the PS. When both populations meet at the mid-streak stage, they establish a completely functional GO (Izpisúa-Belmonte et al., 1993; Streit et al., 2000; Joubin and Stern, 2001). As in *Xenopus* and unlike in mice, Chrd expression in chick embryos begins before the onset of gastrulation (Fig. 7G). Transcripts are initially found in a region just anterior to KS in the epiblast and the underlying cells of the middle layer. Therefore, it is expressed in both populations that contribute to the GO (Streit et al., 1998) (Fig. 7G). A rough fate map of the early blastula/pre-streak chick embryo showed that the prospective forebrain position lies in the epiblast, also immediately anterior to the KS (Stern et al., 2006) (Fig. 7H), suggesting that Chrd is also transiently expressed in the chick forebrain precursors, like in the *Xenopus* BCNE at equivalent stages (as suggested by Kuroda et al., 2004; Reversade et al., 2005) (Fig. 7G). Ectopic expression of Chrd in the non-neural ectoderm of the area pellucida in gastrulating chick embryos was unable to induce a secondary PS or neural markers. However, when Chrd was ectopically expressed earlier, in the anterior edge of the area pellucida before the onset of gastrulation, a secondary axis with PS, node, and neural ectoderm with the typical horseshoe shape of the anterior neural plate was induced (Streit et al., 1998). This suggests that forebrain precursors are competent to be recruited by Chrd before the onset of gastrulation in chick embryos.

In pre-streak chick embryos (stage XII/XIII), Nodal is expressed in a region confined to the middle two-thirds of KS, while Chrd expression is restricted to the midline region of the epiblast, just rostral to KS (Lawson et al., 2001) (Fig. 7G). Therefore, as in *Xenopus*, Nodal is expressed in the chick NC equivalent. Nodal alone was insufficient to induce ectopic Chrd in explants of anterior epiblast of pre-streak embryos but could induce it when combined with FGF8. On the other hand, in the absence of FGF8 signaling, Nodal expression remained unaffected in posterior blastoderm explants (containing KS) of pre-streak embryos, while Chrd expression was decreased (Matsui et al., 2008). These results indicate that FGF8 signaling from the nascent hypoblast is necessary for Chrd expression before the onset of avian gastrulation and that Nodal might cooperate but is insufficient to induce it. However, experiments blocking Nodal were not performed to address if it is indeed required for triggering Chrd expression in the posterior epiblast before gastrulation.

In Zebrafish, *chrd* is readily detected well before gastrulation in the dorsal region, including the future GO region and extending more or less towards the animal pole, depending on the bibliography (Miller-Bertoglio et al., 1997; Sidi et al., 2003; Branam et al., 2010) (Fig. 7D). In contrast to the other vertebrate models discussed here, *chrd* is additionally expressed during gastrulation in territories beyond the GO, including the prospective brain and other neuroectodermal regions (Miller-Bertoglio et al., 1997; Sidi et al., 2003; Branam et al., 2010) (Fig. 7E,F). Notably, in double mutants for *nodal1* and *nodal2* (squint/cyclops) or in maternal/zygotic mutants for the essential cofactor for Nodal signaling *tdgf1* (*MZoep* mutants), the *chrd* domain in the dorsal center of the zebrafish blastula was reduced in size, but strong expression persisted in a considerable subdomain (Gritsman et al., 1999). Also, at blastula stages, *tbxt* expression was suppressed in the dorsal region but persisted in the remaining presumptive mesodermal ring, while *gsc* expression was suppressed in these mutants (Feldman et al., 1998; Gritsman et al., 1999). These observations indicate that the population of *chrd*+ cells in the zebrafish blastula is also heterogeneous in Nodal requirements, as we found in *Xenopus* (this work). They also show that the CM precursors (as we found in *Xenopus*) as well as the PM precursors (unlike what we observed in *Xenopus*) require Nodal signaling for their initial specification (Fig. 7D). As both PM and CM markers were suppressed at blastula stages, the *chrd*+ cells that remain in these mutants might as well represent future neural cells.

Interestingly, zebrafish has a *chordin-like2* (*chrdl2*) gene which also behaves as a BMP antagonist. The zebrafish ortholog of the *chrdl1* gene could not be identified in the genome (Branam et al., 2010). *Chrdl2* is strongly expressed throughout the animal hemisphere before gastrulation (Fig. 7D), thus introducing an additional level of BMP antagonism to the dorsal region. Knockdown experiments showed that *chrl2* is required together with *chrd* for dorsal development during the patterning of the embryonic dorsal-ventral axis (Branam et al., 2010).

Concluding remarks

The rostral forebrain is an evolutionary acquisition of vertebrates related to the appearance of the Hesx1 gene at the beginning of vertebrate evolution (Ermakova et al., 1999; Wilson and Houart, 2004; Ermakova et al., 2007; Bayramov et al., 2016) and derives entirely from the BCNE center (Kuroda et al., 2004). We have previously shown that expression of the rostral forebrain regulator *hesx1* persists after blocking Nodal signaling in *Xenopus* (Murgan et al., 2014). Indeed, the expansion of the Hesx1 domain in Nodal$^{-/-}$ mouse embryos occurred before gastrulation (Camus et al., 2006). Altogether, our findings and the comparison between different vertebrate models indicate that the establishment of the CNS during the development of vertebrates requires not only a very early

induction of the brain territory but also its delimitation. This process involves Nodal signaling in the differential segregation of the cell populations that give rise to the dorsal structures (brain and AM) as early as at the onset of neural induction at the blastula stage.

MATERIALS AND METHODS

Embryological manipulations, mRNA synthesis, and injections

Albino and wild-type *Xenopus laevis* embryos were obtained by natural mating or by *in vitro* fertilization using standard methods (Sive et al., 2010) and staged according to (Nieuwkoop and Faber, 1994). Parental animals were obtained from Nasco (Fort Atkinson, WI, USA). Protocols were approved by the Laboratory Animal Welfare and Research Committee (CICUAL) from Facultad de Medicina-UBA.

To obtain synthetic capped mRNAs, the following plasmids were employed as templates: *Xcer-S pCS2+* (gift from Eddy de Robertis, University of California, LA, USA) (Bouwmeester et al., 1996), *pCS2 MT foxH1-SID* [gift from Uwe Strähle, European Zebrafish Resource Center (EZRC), Karlsruhe, Germany] (Chen et al., 1997), and *pCS2-NLS-lacZ* (gift from Tomas Pieler, Department of Developmental Biochemistry, University of Goettingen, Germany) (Bellefroid et al., 1996). These plasmids were linearized with NotI and transcribed with SP6 mRNA polymerase with the mMESSAGE mMACHINE SP6 Transcription Kit (Thermo Fisher Scientific, AM1340), following the manufacturer's instructions. Synthetic capped mRNAs were purified with the RNeasy Mini Kit (Qiagen, #74104).

Microinjection, culture, and fixation of embryos were performed as previously described (Murgan et al., 2014). *Cer-S* mRNA was injected in the vegetal region of the four cells at s3 (0.5 ng/cell). *Foxh1-SID* mRNA (0.25 to 1 ng) was unilaterally injected at s2. Microinjections included as tracer 30–40 ng/cell of Dextran Oregon Green 488, MW 10000, anionic, lysine fixable (DOG; Thermo Fisher Scientific, D7171) or of Dextran Alexa Fluor 594, MW 10000, anionic, fixable (Thermo Fisher Scientific, D22913); or 0.5 ng/cell of *nuc-lacZ* mRNA.

ISH and X-gal staining

Plasmids for obtaining antisense RNA probes for wholemount ISH were linearized and transcribed as follows. *Chrd1: pSB59-chrd1* (gift from Eddy de Robertis) (Sasai et al., 1994) was cut with EcoRI and transcribed with T7 RNA polymerase; *Gsc*: *gsc pG500* (gift from Ken Cho, University of California, Irvine, CA, USA) (Cho et al., 1991), XbaI/T3; *myod1: pSP73-XmyoD* (gift from Cristof Niehrs, Institute of Molecular Biology, Mainz, Germany) (Hopwood et al., 1989), BamHI/SP6; *not: pBS-KS-Xnot:* HindIII/T7 (gift from David Kimelman, Department of Biochemistry, University of Washington, Seattle, WA, USA) (von Dassow et al., 1993); *sia1: pBluescript RN3 Xsia ORF* (gift from Patrick Lemaire, Institut de Biologie du Developpement de Marseille, Marseille, France) (Lemaire et al., 1995), HindIII/T7; *sox2: pBS sox2* (gift from Yoshiki Sasai, RIKEN Center for Developmental Biology, Kobe, Japan) (Kishi et al., 2000), EcoRI/T7; *tbxt: αpSP64T bra* (gift from Abraham Fainsod, Faculty of Medicine, The Autism Centre Hebrew University, Jerusalem, Israel) (Smith et al., 1991), SalI/SP6. The preparation of digoxigenin-labeled antisense RNA probes and the wholemount ISH procedure was performed as previously described (Pizard et al., 2004), except that the proteinase K step was omitted. X-gal staining for revealing the *nuc-lacZ* tracer was performed as previously described (Franco et al., 1999).

RT-qPCR analysis

Embryos injected with *cer-S* mRNA and uninjected siblings were allowed to grow until stages 9 or 10. For total RNA extraction, three embryos at s9 or eight embryos at s10 were placed in 1.5 ml tubes. After liquid withdrawal, tubes were placed on ice, and 200 µl (for s9 samples) or 400 µl (for s10 samples) of TRIreagent (Merck, cat. no. 93289) was added. Embryos were resuspended 10 times with a micropipette. Samples were stored at −80°C until RNA extraction, which was performed following the manufacturer's instructions. 1 µg of RNA was treated with DNAse I (Ambion, cat. no. AM2222) and used for first-strand cDNA synthesis, using High Capacity Reverse Transcription Kit with random primers (Applied Biosystems, cat no. 4368814). Amplification was performed in triplicate in an Applied Biosystems 7500 Real-Time PCR System machine using Power Up SYBR Green Master Mix (Applied Biosystems, cat. no. A25472). Melt curves were analyzed to confirm the specificity of PCR products. The efficiency of each PCR amplification was estimated using the slope of a standard curve. Relative gene expression was calculated using Pfaffl′s mathematical model, with Histone H4 expression levels as standard.

The following primers were used for RT-qPCR: *chrd.1* F: ACTGCCAGGACTGGATGGT, *chrd.1* R: GGCAGGATTTAGAGTTGC-TTC (Leibovich et al., 2018); *gsc F:* TTCACCGATGAACAACTGGA, *gsc R:* TTCCACTTTTGGGCATTTTC (Leibovich et al., 2018); *histone H4* F: GGCAAAGGAGGAAAAGGACTG, *histone H4* R: GGTGATGCCCTG-GATGTTGT (Cao et al., 2007); *mix1* F: CAAAAGCCACCAAGCCCATT, *mix1* R: TGCTGAAGGAAACATTGCCC (Sun et al., 2015); *sox2* F: GA-GGATGGACACTTATGCCCAC, *sox2* R: GGACATGCTGTAGGTAGG-CGA E.M. (De Robertis http://www.hhmi.ucla.edu/derobertis/).

Data collection and statistics

Cer-S mRNA batches for ISH analysis were tested by the effect on the mesodermal marker *myod1* at neurula stage and were used when *myod1* expression was strongly attenuated or abolished in injected embryos in comparison to uninjected siblings (Fig. S1C,D; Table 1). *Fox1-SID* mRNA was tested by the effect on the pan-mesodermal marker *tbxt* at early gastrula stage by ISH analysis (Fig. S1E–G). For RT-qPCR analysis, *cer-S* mRNA-injected batches were tested at s9 and s10 by the effect on the expression of *mix1*, a direct target of Nodal signaling (Charney et al., 2017), and were used when *mix1* expression was significantly reduced to less than 50% in relation to uninjected sibling controls (Fig. S1A,B).

The numbers of samples (n) and biological replicates (N) that were analyzed are indicated for each set of experiments in the figures and tables. Biological replicates represent batches of embryos from independent mating pairs, or from different groups of embryos from the same batch in the case of RT-qPCR assays at s9. Statistical tests applied for RT-qPCR analysis are described in the corresponding Materials and Methods section and the figures. Differences were considered significant when $P<0.05$.

Acknowledgements

We thank the following colleagues for providing us with DNAs: Ken Cho (*gsc*), Eddy De Robertis (*chrd.1*, *cer-S*), Abraham Fainsod (*tbxt*), Tomas Pieler (NLS-lacZ/*nuc-lacZ*), David Kimelman (*not*), Patrick Lemaire (*sia1*), Christof Niehrs (*myod1*), Yoshiki Sasai (*sox2*), and Uwe Strähle (*foxh1-SID*). We are grateful to Marianela Ceol Retamal, Andrea Pecile, Manuel Ponce, and Ezequiel Yamus for animal husbandry, and to María Belén Favarolo for help with experiments.

Competing interests

The authors declare no competing or financial interests.

Author contributions

Conceptualization: A.M.C.C., S.L.L.; Formal analysis: A.M.C.C., M.B.T., L.E.B.L., S.L.L.; Investigation: A.M.C.C., M.B.T., L.E.B.L., S.L.L.; Resources: M.R., L.F.F., S.L.L.; Writing - original draft: A.M.C.C., S.L.L.; Writing - review & editing: A.M.C., M.R., L.F.F., S.L.L.; Visualization: A.M.C., M.B.T., S.L.L.; Supervision: S.L.L.; Project administration: S.L.L.; Funding acquisition: S.L.L.

Funding

Research was supported by Agencia Nacional de Promoción Científica y Tecnológica, Argentina (PICT 2011-1559, PICT 2014-2020) and Consejo Nacional de Investigaciones Científicas y Técnicas, Argentina (PIP 2012-0508, PIP 2015-0577; fellowship to A.M.C.C.).

Supplementary information

Supplementary information available online at
https://bio.biologists.org/lookup/doi/10.1242/bio.051797.supplemental

References

Agius, E., Oelgeschläger, M., Wessely, O., Kemp, C. and De Robertis, E. M. (2000). Endodermal Nodal-related signals and mesoderm induction in Xenopus. *Development* **127**, 1173-1183.

Aguirre, C. E., Murgan, S., Carrasco, A. E. and López, S. L. (2013). An intact brachyury function is necessary to prevent spurious axial development in Xenopus laevis. *PLoS ONE* **8**, e54777. doi:10.1371/journal.pone.0054777

Anderson, R. M., Lawrence, A. R., Stottmann, R. W., Bachiller, D. and Klingensmith, J. (2002). Chordin and noggin promote organizing centers of forebrain development in the mouse. *Development* **129**, 4975-4987.
Artinger, M., Blitz, I., Inoue, K., Tran, U. and Cho, K. W. Y. (1997). Interaction of goosecoid and brachyury in Xenopus mesoderm patterning. *Mech. Dev.* **65**, 187-196. doi:10.1016/S0925-4773(97)00073-7
Bachiller, D., Klingensmith, J., Kemp, C., Belo, J. A., Anderson, R. M., May, S. R., McMahon, J. A., McMahon, A. P., Harland, R. M., Rossant, J. et al. (2000). The organizer factors Chordin and Noggin are required for mouse forebrain development. *Nature* **403**, 658-661. doi:10.1038/35001072
Bauer, D. V., Huang, S. and Moody, S. A. (1994). The cleavage stage origin of Spemann's Organizer: analysis of the movements of blastomere clones before and during gastrulation in Xenopus. *Development* **120**, 1179-1189.
Bayramov, A. V., Ermakova, G. V., Eroshkin, F. M., Kucheryavyy, A. V., Martynova, N. Y. and Zaraisky, A. G. (2016). The presence of Anf/Hesx1 homeobox gene in lampreys suggests that it could play an important role in emergence of telencephalon. *Sci. Rep.* **6**, 39849. doi:10.1038/srep39849
Beddington, R. S. and Robertson, E. J. (1999). Axis development and early asymmetry in mammals. *Cell* **96**, 195-209. doi:10.1016/S0092-8674(00)80560-7
Bellefroid, E. J., Bourguignon, C., Hollemann, T., Ma, Q., Anderson, D. J., Kintner, C. and Pieler, T. (1996). X-MyT1, a Xenopus C2HC-type zinc finger protein with a regulatory function in neuronal differentiation. *Cell* **87**, 1191-1202. doi:10.1016/S0092-8674(00)81815-2
Blanco-Suarez, E., Liu, T.-F., Kopelevich, A. and Allen, N. J. (2018). Astrocyte-secreted chordin-like 1 drives synapse maturation and limits plasticity by increasing synaptic GluA2 AMPA receptors. *Neuron* **100**, 1116-1132.e13. doi:10.1016/j.neuron.2018.09.043
Bouwmeester, T., Kim, S., Sasai, Y., Lu, B. and De Robertis, E. M. (1996). Cerberus is a head-inducing secreted factor expressed in the anterior endoderm of Spemann's organizer. *Nature* **382**, 595-601. doi:10.1038/382595a0
Branam, A. M., Hoffman, G. G., Pelegri, F. and Greenspan, D. S. (2010). Zebrafish chordin-like and chordin are functionally redundant in regulating patterning of the dorsoventral axis. *Dev. Biol.* **341**, 444-458. doi:10.1016/j.ydbio.2010.03.001
Camus, A., Perea-Gomez, A., Moreau, A. and Collignon, J. (2006). Absence of Nodal signaling promotes precocious neural differentiation in the mouse embryo. *Dev. Biol.* **295**, 743-755. doi:10.1016/j.ydbio.2006.03.047
Cao, Y., Siegel, D., Donow, C., Knöchel, S., Yuan, L. and Knöchel, W. (2007). POU-V factors antagonize maternal VegT activity and beta-Catenin signaling in Xenopus embryos. *EMBO J.* **26**, 2942-2954. doi:10.1038/sj.emboj.7601736
Chandra, A., Itakura, T., Yang, Z., Tamakoshi, T., Xue, X. D., Wang, B., Ueki, T., Sato, K., Uezato, T. and Miura, N. (2006). Neurogenesin-1 differentially inhibits the osteoblastic differentiation by bone morphogenetic proteins in C2C12 cells. *Biochem. Biophys. Res. Commun.* **344**, 786-791. doi:10.1016/j.bbrc.2006.03.195
Charney, R. M., Paraiso, K. D., Blitz, I. L. and Cho, K. W. Y. (2017). A gene regulatory program controlling early Xenopus mesendoderm formation: Network conservation and motifs. *Semin. Cell Dev. Biol.* **66**, 12-24. doi:10.1016/j.semcdb.2017.03.003
Chen, X., Weisberg, E., Fridmacher, V., Watanabe, M., Naco, G. and Whitman, M. (1997). Smad4 and FAST-1 in the assembly of activin-responsive factor. *Nature* **389**, 85-89. doi:10.1038/38008
Cho, K. W. Y., Blumberg, B., Steinbeisser, H. and De Robertis, E. M. (1991). Molecular nature of Spemann's organizer: the role of the Xenopus homeobox gene goosecoid. *Cell* **67**, 1111-1120. doi:10.1016/0092-8674(91)90288-A
Coffinier, C., Tran, U., Larraín, J. and De Robertis, E. M. (2001). Neuralin-1 is a novel Chordin-related molecule expressed in the mouse neural plate. *Mech. Dev.* **100**, 119-122. doi:10.1016/S0925-4773(00)00507-4
Conlon, F. L., Lyons, K. M., Takaesu, N., Barth, K. S., Kispert, A., Herrmann, B. and Robertson, E. J. (1994). A primary requirement for nodal in the formation and maintenance of the primitive streak in the mouse. *Development* **120**, 1919-1928.
De Robertis, E. M. and Kuroda, H. (2004). Dorsal-ventral patterning and neural induction in Xenopus embryos. *Annu. Rev. Cell Dev. Biol.* **20**, 285-308. doi:10.1146/annurev.cellbio.20.011403.154124
Ermakova, G. V., Solovieva, E. A., Martynova, N. Y. and Zaraisky, A. G. (2007). The homeodomain factor Xanf represses expression of genes in the presumptive rostral forebrain that specify more caudal brain regions. *Dev. Biol.* **307**, 483-497. doi:10.1016/j.ydbio.2007.03.524
Ermakova, G. V., Alexandrova, E. M., Kazanskaya, O. V., Vasiliev, O. L., Smith, M. W. and Zaraisky, A. G. (1999). The homeobox gene, Xanf-1, can control both neural differentiation and patterning in the presumptive anterior neurectoderm of the Xenopus laevis embryo. *Development* **126**, 4513-4523.
Feldman, B., Gates, M. A., Egan, E. S., Dougan, S. T., Rennebeck, G., Sirotkin, H. I., Schier, A. F. and Talbot, W. S. (1998). Zebrafish organizer development and germ-layer formation require nodal-related signals. *Nature* **395**, 181-185. doi:10.1038/26013
Foley, A. C., Skromne, I. and Stern, C. D. (2000). Reconciling different models of forebrain induction and patterning: a dual role for the hypoblast. *Development* **127**, 3839-3854.
Franco, P. G., Paganelli, A. R., López, S. L. and Carrasco, A. E. (1999). Functional association of retinoic acid and hedgehog signaling in Xenopus primary neurogenesis. *Development* **126**, 4257-4265.
Gritsman, K., Zhang, J., Cheng, S., Heckscher, E., Talbot, W. S. and Schier, A. F. (1999). The EGF-CFC protein one-eyed pinhead is essential for nodal signaling. *Cell* **97**, 121-132. doi:10.1016/S0092-8674(00)80720-5
Harata, A., Hirakawa, M., Sakuma, T., Yamamoto, T. and Hashimoto, C. (2019). Nucleotide receptor P2RY4 is required for head formation via induction and maintenance of head organizer in Xenopus laevis. *Dev. Growth Differ.* **61**, 186-197. doi:10.1111/dgd.12563
Hausen, P. and Riebesell, M. (1991). *The Early Development of Xenopus Laevis: An Atlas of Histology*. Berlin, Heidelberg, New York: Springer-Verlag.
Hill, C. S. (2001). TGF-β signalling pathways in early Xenopus development. *Curr. Opin. Genet. Dev.* **11**, 533-540. doi:10.1016/S0959-437X(00)00229-X
Hoodless, P. A., Pye, M., Chazaud, C., Labbé, E., Attisano, L., Rossant, J. and Wrana, J. L. (2001). FoxH1 (Fast) functions to specify the anterior primitive streak in the mouse. *Genes Dev.* **15**, 1257-1271. doi:10.1101/gad.881501
Hopwood, N. D., Pluck, A. and Gurdon, J. B. (1989). MyoD expression in the forming somites is an early response to mesoderm induction in Xenopus embryos. *EMBO J.* **8**, 3409-3417. doi:10.1002/j.1460-2075.1989.tb08505.x
Ishibashi, H., Matsumura, N., Hanafusa, H., Matsumoto, K., De Robertis, E. M. and Kuroda, H. (2008). Expression of Siamois and Twin in the blastula Chordin/Noggin signaling center is required for brain formation in Xenopus laevis embryos. *Mech. Dev.* **125**, 58-66. doi:10.1016/j.mod.2007.10.005
Izpisúa-Belmonte, J. C., De Robertis, E. M., Storey, K. G. and Stern, C. D. (1993). The homeobox gene goosecoid and the origin of organizer cells in the early chick blastoderm. *Cell* **74**, 645-659. doi:10.1016/0092-8674(93)90512-O
Joubin, K. and Stern, C. D. (2001). Formation and maintenance of the organizer among the vertebrates. *Int. J. Dev. Biol.* **45**, 165-175.
Kaneda, T. and Motoki, J.-Y. D. (2012). Gastrulation and pre-gastrulation morphogenesis, inductions, and gene expression: Similarities and dissimilarities between urodelean and anuran embryos. *Development* **369**, 1-18. doi:10.1016/j.ydbio.2012.05.019
Keller, R. E. (1975). Vital dye mapping of the gastrula and neurula of Xenopus laevis. *Dev. Biol.* **42**, 222-241. doi:10.1016/0012-1606(75)90331-0
Keller, R. E. (1976). Vital dye mapping of the gastrula and neurula of Xenopus laevis. II. Prospective areas and morphogenetic movements of the deep layer. *Dev. Biol.* **51**, 118-137. doi:10.1016/0012-1606(76)90127-5
Kinder, S. J., Tsang, T. E., Wakamiya, M., Sasaki, H., Behringer, R. R., Nagy, A. and Tam, P. P. L. (2001). The organizer of the mouse gastrula is composed of a dynamic population of progenitor cells for the axial mesoderm. *Development* **128**, 3623-3634.
Kishi, M., Mizuseki, K., Sasai, N., Yamazaki, H., Shiota, K., Nakanishi, S. and Sasai, Y. (2000). Requirement of Sox2-mediated signaling for differentiation of early Xenopus neuroectoderm. *Development* **127**, 791-800.
Kuroda, H., Wessely, O. and De Robertis, E. M. (2004). Neural induction in Xenopus: requirement for ectodermal and endomesodermal signals via Chordin, Noggin, β-Catenin, and Cerberus. *PLoS Biol.* **2**, E92. doi:10.1371/journal.pbio.0020092
Kurth, T., Meissner, S., Schäckel, S. and Steinbeisser, H. (2005). Establishment of mesodermal gene expression patterns in early Xenopus embryos: the role of repression. *Dev. Dyn.* **233**, 418-429. doi:10.1002/dvdy.20342
Kwan, K. M. and Kirschner, M. W. (2003). Xbra functions as a switch between cell migration and convergent extension in the Xenopus gastrula. *Development* **130**, 1961-1972. doi:10.1242/dev.00412
Latinkić, B. V. and Smith, J. C. (1999). Goosecoid and mix.1 repress Brachyury expression and are required for head formation in Xenopus. *Development* **126**, 1769-1779.
Lawson, A., Colas, J. F. and Schoenwolf, G. C. (2001). Classification scheme for genes expressed during formation and progression of the avian primitive streak. *Anat. Rec.* **262**, 221-226. doi:10.1002/1097-0185(20010201)262:2<221::AID-AR1019>3.0.CO;2-F
Leibovich, A., Kot-Leibovich, H., Ben-Zvi, D. and Fainsod, A. (2018). ADMP controls the size of Spemann's organizer through a network of self-regulating expansion-restriction signals. *BMC Biol.* **16**, 13. doi:10.1186/s12915-018-0483-x
Lemaire, P., Garrett, N. and Gurdon, J. B. (1995). Expression cloning of Siamois, a Xenopus homeobox gene expressed in dorsal-vegetal cells of blastulae and able to induce a complete secondary axis. *Cell* **81**, 85-94. doi:10.1016/0092-8674(95)90373-9
Levine, A. J. and Brivanlou, A. H. (2007). Proposal of a model of mammalian neural induction. *Dev. Biol.* **308**, 247-256. doi:10.1016/j.ydbio.2007.05.036
Luu, O., Nagel, M., Wacker, S., Lemaire, P. and Winklbauer, R. (2008). Control of gastrula cell motility by the Goosecoid/Mix.1/ Siamois network: basic patterns and paradoxical effects. *Dev. Dyn.* **237**, 1307-1320. doi:10.1002/dvdy.21522
Matsui, H., Sakabe, M., Sakata, H., Yanagawa, N., Ikeda, K., Yamagishi, T. and Nakajima, Y. (2008). Induction of initial heart α-actin, smooth muscle α-actin, in chick pregastrula epiblast: The role of hypoblast and fibroblast growth factor-8. *Dev. Growth Differ.* **50**, 143-157. doi:10.1111/j.1440-169X.2008.00987.x
McMahon, J. A., Takada, S., Zimmerman, L. B., Fan, C.-M., Harland, R. M. and McMahon, A. P. (1998). Noggin-mediated antagonism of BMP signaling is

required for growth and patterning of the neural tube and somite. *Genes Dev.* **12**, 1438-1452. doi:10.1101/gad.12.10.1438

Miller-Bertoglio, V. E., Fisher, S., Sánchez, A., Mullins, M. C. and Halpern, M. E. (1997). Differential regulation of chordin expression domains in mutant zebrafish. *Dev. Biol.* **192**, 537-550. doi:10.1006/dbio.1997.8788

Müller, F., Albert, S., Blader, P., Fischer, N., Hallonet, M. and Strähle, U. (2000). Direct action of the nodal-related signal cyclops in induction of sonic hedgehog in the ventral midline of the CNS. *Development* **127**, 3889-3897.

Murgan, S., Castro Colabianchi, A. M., Monti, R. J., Boyadjián López, L. E., Aguirre, C. E., Stivala, E. G., Carrasco, A. E. and López, S. L. (2014). FoxA4 Favours notochord formation by inhibiting contiguous mesodermal fates and restricts anterior neural development in Xenopus embryos. *PLoS ONE* **9**, e110559. doi:10.1371/journal.pone.0110559

Nieuwkoop, P. D. and Faber, J. (1994). *Normal Table of Xenopus Laevis (Daudin)*. New York and London: Garland Publishing.

Pfirrmann, T., Emmerich, D., Ruokonen, P., Quandt, D., Buchen, R., Fischer-Zirnsak, B., Hecht, J., Krawitz, P., Meyer, P., Klopocki, E. et al. (2014). Molecular mechanism of CHRDL1-mediated X-linked megalocornea in humans and in Xenopus model. *Hum. Mol. Genet.* **24**, 3119-3132. doi:10.1093/hmg/ddv063

Piccolo, S., Agius, E., Leyns, L., Bhattacharyya, S., Grunz, H., Bouwmeester, T. and De Robertis, E. M. (1999). The head inducer Cerberus is a multifunctional antagonist of Nodal, BMP and Wnt signals. *Nature* **397**, 707-710. doi:10.1038/17820

Pizard, A., Haramis, A., Carrasco, A. E., Franco, P., López, S. and Paganelli, A. (2004). Whole-mount in situ hybridization and detection of RNAs in vertebrate embryos and isolated organs. *Curr. Protoc. Mol. Biol.* **Chapter 14**, Unit 9. doi:10.1002/0471142727.mb1409s66

Rebagliati, M. R., Toyama, R., Fricke, C., Haffter, P. and Dawid, I. B. (1998). Zebrafish nodal-related genes are implicated in axial patterning and establishing left-right asymmetry. *Dev. Biol.* **199**, 261-272. doi:10.1006/dbio.1998.8935

Reid, C. D., Zhang, Y., Sheets, M. D. and Kessler, D. S. (2012). Transcriptional integration of Wnt and Nodal pathways in establishment of the Spemann organizer. *Dev. Biol.* **368**, 231-241. doi:10.1016/j.ydbio.2012.05.018

Reid, C. D., Steiner, A. B., Yaklichkin, S., Lu, Q., Wang, S., Hennessy, M. and Kessler, D. S. (2016). FoxH1 mediates a Grg4 and Smad2 dependent transcriptional switch in Nodal signaling during Xenopus mesoderm development. *Dev. Biol.* **414**, 34-44. doi:10.1016/j.ydbio.2016.04.006

Reversade, B., Kuroda, H., Lee, H., Mays, A. and De Robertis, E. M. (2005). Depletion of Bmp2, Bmp4, Bmp7 and Spemann organizer signals induces massive brain formation in Xenopus embryos. *Development* **132**, 3381-3392. doi:10.1242/dev.01901

Sakuta, H., Suzuki, R., Takahashi, H., Kato, A., Shintani, T., Iemura Si, Yamamoto, T. S., Ueno, N. and Noda, M. (2001). Ventroptin: a BMP-4 antagonist expressed in a double-gradient pattern in the retina. *Science* **293**, 111-115. doi:10.1126/science.1058379

Sasai, Y., Lu, B., Steinbeisser, H., Geissert, D., Gont, L. K. and De Robertis, E. M. (1994). Xenopus chordin: a novel dorsalizing factor activated by organizer-specific homeobox genes. *Cell* **79**, 779-790. doi:10.1016/0092-8674(94)90068-X

Schohl, A. and Fagotto, F. (2002). Beta-catenin, MAPK and Smad signaling during early Xenopus development. *Development* **129**, 37-52.

Shen, M. M. (2007). Nodal signaling: development roles and regulation. *Development* **134**, 1023-1034. doi:10.1242/dev.000166

Shook, D. and Keller, R. (2004). Gastrulation in amphibians. In *Gastrulation: From Cells to Embryo* (ed. C. D. Stern), pp. 171-203. Cold Spring Harbor Laboratory Press.

Shook, D. R., Majer, C. and Keller, R. (2004). Pattern and morphogenesis of presumptive superficial mesoderm in two closely related species, Xenopus laevis and Xenopus tropicalis. *Dev. Biol.* **270**, 163-185. doi:10.1016/j.ydbio.2004.02.021

Sidi, S., Goutel, C., Peyriéras, N. and Rosa, F. M. (2003). Maternal induction of ventral fate by zebrafish radar. *Proc. Natl. Acad. Sci. USA* **100**, 3315-3320. doi:10.1073/pnas.0530115100

Sive, H. L., Grainger, R. M. and Harland, R. M. (2010). Early Development of Xenopus laevis. A Laboratory Manual. Cold Spring Harbor: Cold Spring Harbor Laboratory Press.

Smith, J. C., Price, B. M. J., Green, J. B. A., Weigel, D. and Herrmann, B. G. (1991). Expression of a Xenopus homolog of Brachyury (T) is an immediate-early response to mesoderm induction. *Cell* **67**, 79-87. doi:10.1016/0092-8674(91)90573-H

Spemann, H. and Mangold, H. (1924). Über Induktion von Embryonalanlagen durch Implantation artfremder Organisatoren. Arch. für Mikroskopische Anat. und Entwicklungsmechanik 100, 599–638.

Stern, C. D. (1990). The marginal zone and its contribution to the hypoblast and primitive streak of the chick embryo. *Development* **109**, 667-682.

Stern, C. D., Charité, J., Deschamps, J., Duboule, D., Durston, A. J., Kmita, M., Nicolas, J.-F., Palmeirim, I., Smith, J. C. and Wolpert, L. (2006). Head-tail patterning of the vertebrate embryo: one, two or many unresolved problems? *Int. J. Dev. Biol.* **50**, 3-15. doi:10.1387/ijdb.052095cs

Streit, A., Lee, K. J., Woo, I., Roberts, C., Jessell, T. M. and Stern, C. D. (1998). Chordin regulates primitive streak development and the stability of induced neural cells, but is not sufficient for neural induction in the chick embryo. *Development* **125**, 507-519.

Streit, A., Berliner, A. J., Papanayotou, C., Sirulnik, A. and Stern, C. D. (2000). Initiation of neural induction by FGF signalling before gastrulation. *Nature* **406**, 74-78. doi:10.1038/35017617

Sudou, N., Yamamoto, S., Ogino, H. and Taira, M. (2012). Dynamic in vivo binding of transcription factors to cis-regulatory modules of cer and gsc in the stepwise formation of the Spemann-Mangold organizer. *Development* **139**, 1651-1661. doi:10.1242/dev.068395

Sun, G., Hu, Z., Min, Z., Yan, X., Guan, Z., Su, H., Fu, Y., Ma, X., Chen, Y.-G., Zhang, M. Q. et al. (2015). Small C-terminal domain phosphatase 3 Dephosphorylates the linker sites of receptor-regulated Smads (R-Smads) to ensure transforming growth factor β (TGFβ)-mediated germ layer induction in Xenopus embryos. *J. Biol. Chem.* **290**, 17239-17249. doi:10.1074/jbc.M115.655605

Takahashi, S., Yokota, C., Takano, K., Tanegashima, K., Onuma, Y., Goto, J. and Asashima, M. (2000). Two novel nodal-related genes initiate early inductive events in Xenopus Nieuwkoop center. *Development* **127**, 5319-5329.

Tam, P. P. L. and Behringer, R. R. (1997). Mouse gastrulation: the formation of a mammalian body plan. *Mech. Dev.* **68**, 3-25. doi:10.1016/S0925-4773(97)00123-8

Tam, P. P. L. and Rossant, J. (2003). Mouse embryonic chimeras: tools for studying mammalian development. *Development* **130**, 6155-6163. doi:10.1242/dev.00893

Tam, P. P., Parameswaran, M., Kinder, S. J. and Weinberger, R. P. (1997). The allocation of epiblast cells to the embryonic heart and other mesodermal lineages: the role of ingression and tissue movement during gastrulation. *Development* **124**, 1631-1642.

Varlet, I., Collignon, J. and Robertson, E. J. (1997). Nodal expression in the primitive endoderm is required for specification of the anterior axis during mouse gastrulation. *Development* **124**, 1033-1044.

Vincent, S. D., Dunn, N. R., Hayashi, S., Norris, D. P. and Robertson, E. J. (2003). Cell fate decisions within the mouse organizer are governed by graded Nodal signals. *Genes Dev.* **17**, 1646-1662. doi:10.1101/gad.1100503

von Dassow, G., Schmidt, J. E. and Kimelman, D. (1993). Induction of the Xenopus organizer: expression and regulation of Xnot, a novel FGF and activin-regulated homeo box gene. *Genes Dev.* **7**, 355-366. doi:10.1101/gad.7.3.355

Watanabe, M. and Whitman, M. (1999). FAST-1 is a key maternal effector of mesoderm inducers in the early Xenopus embryo. *Development* **126**, 5621-5634.

Wessely, O., Agius, E., Oelgeschläger, M., Pera, E. M. and De Robertis, E. M. (2001). Neural induction in the absence of mesoderm: beta-catenin-dependent expression of secreted BMP antagonists at the blastula stage in Xenopus. *Dev. Biol.* **234**, 161-173. doi:10.1006/dbio.2001.0258

Wilson, S. W. and Houart, C. (2004). Early steps in the development of the forebrain. *Dev. Cell.* **6**, 167-181. doi:10.1016/S1534-5807(04)00027-9

Yamaguchi, T. P. (2001). Heads or tails: Wnts and anterior-posterior patterning. Curr. Biol. 11, R713-24. doi:10.1016/S0960-9822(01)00417-1

Yamaguti, M., Cho, K. W. Y. and Hashimoto, C. (2005). Xenopus hairy2b specifies anterior prechordal mesoderm identity within Spemann's organizer. *Dev. Dyn.* **234**, 102-113. doi:10.1002/dvdy.20523

Yamamoto, M., Meno, C., Sakai, Y., Shiratori, H., Mochida, K., Ikawa, Y., Saijoh, Y. and Hamada, H. (2001). The transcription factor FoxH1 (FAST) mediates Nodal signaling during anterior-posterior patterning and node formation in the mouse. *Genes Dev.* **15**, 1242-1256. doi:10.1101/gad.883901

Zorn, A. M., Butler, K. and Gurdon, J. B. (1999). Anterior endomesoderm specification in Xenopus by Wnt/β-catenin and TGF-β signalling pathways. *Dev. Biol.* **209**, 282-297. doi:10.1006/dbio.1999.9257